

CHAPTER 1

ACOUSTICAL SIGNALS OF BIOMECHANICAL SYSTEMS

EUGENIJUS KANIUSAS

*Institute of Fundamentals and Theory of Electrical Engineering,
Bioelectricity & Magnetism Lab, Vienna University of Technology,
Gusshausstrasse 27-29/E351, A-1040 Vienna, Austria
kaniusas@tuwien.ac.at*

Traditionally, acoustical signals of biomechanical systems show a high clinical relevance when auscultated on the body skin. The heart and lung sounds are applied to the diagnosis of cardiac and respiratory disturbances, respectively, whereas the snoring sounds have been recently acknowledged as important symptoms of the airway obstruction. This chapter aims at the simultaneous consideration of all three types of body sounds from a biomechanical point of view. That is, the respective generation mechanisms are outlined, showing that the vibrations of different tissue structures and air turbulences manifest as regionally concentrated or distributed sound sources. The resulting acoustical properties and mutual interrelations of the body sounds are commented. The investigation of the sound propagation demonstrates an inhomogeneous and frequency-dependant attenuation of sounds within the body, yielding a specific spatial and regional distribution of the sound intensity inside the body and on the body skin (as the auscultation region), respectively. The presented issues pertaining to the biomechanical generation and transmission of the body sounds not only reveal clinically relevant correlations between the physiological phenomena under investigation and the registered biosignals, but also offer a solid basis for both proper understanding of the biosignal relevance and optimization of the recording techniques.

1. Introduction

In many ways, the body sounds of human biomechanical systems have remained timeless since Laennec, inventor of the stethoscope,^a improved the audibility of

^aThe stethoscope (greek *stetos* chest and *skopein* explore) is a basic and widely established medical instrument, viewed by many as the very symbol of medicine, for conduction of the sounds generated inside the body between the body surface and the ears. The auscultation of the body sounds was employed more than 20 centuries ago, as suggested in Hippocrates work “de Morbis”: “If you listen by applying the ear to the chest. . .”.¹ The inventor of the original stethoscope, R. T. H. Laennec, made in 1816 an epoch making observation with a wooden cylinder which was primarily sought to avoid embarrassment. “I was consulted,” says Laennec, “by a young woman who presented some general symptoms of disease of heart. . . On account of the age and sex of the patient, the common modes of exploration (immediate application of the ear) being inapplicable, I was led to recollect a well known acoustic phenomenon. . .” Later, in 1894, A. Bianchi introduced a rigid diaphragm over the part of the cylinder that was applied to the chest. Today, the modern stethoscope consists of a bell-type chestpiece for sound amplification, a rubber tube for sound transmission, and earpieces for conducting the sound into ears.^{2,3}

heart and lung sounds with the stethoscope. These sounds have conveyed meaningful signals to the examiner looking for cardiorespiratory disturbances. Recently, medical interest has also been focused on snoring sounds, the relevance of which has been acknowledged, for instance, as a warning sign that normal breathing is not taking place during sleep or even as the first sign of the sleep apnea syndrome.^b

Obviously the stethoscope has continued to be the most relevant instrument for the auscultation (latin *auscultare* the act of listening) of the body sounds since its invention nearly two centuries ago. A modern version of the stethoscope is shown in Fig. 1, which demonstrates a body sounds sensor, i.e. a chestpiece of the stethoscope combined with a microphone. The chestpiece diaphragm being in close contact with the skin vibrates with the skin which, in turn, follows the vibrations induced by the mechanical forces of the body sounds. The vibrations of the diaphragm create acoustic pressure waves traveling into the bell and further to the microphone. The latter acts as an electro-acoustic converter to establish a body sounds signal s for the signal processing.

The physical properties of the arising acoustic transmission path within the body sounds sensor have strong implications on the transmission characteristics of the body sounds. In particular, the resonant characteristics of the chestpiece (= Helmholtz resonator^{1,7}) play a significant role concerning the non-linear filtering and amplification characteristics of the body sounds sensor.^{1-3,8-10}

2. Body Sounds — An Overview

A brief outline of the body sounds is given below, including their biomechanical generation mechanisms and acoustical properties. In particular, it will be shown that the vibrations of tissues, valves inside the heart, blood, walls of airways, and air turbulences manifest as the body sounds which are accessible through the auscultation on the skin (Fig. 1). From an acoustical point of view, the body sounds are normally impure tones or noises, and therefore are composed of a conglomeration of frequencies of multitudinous intensities. As already mentioned, the body sounds include (Fig. 1)

It is worth mentioning that the introduction of the stethoscope forced physicians to a cardinal reorientation, for the stethoscope had altered the physician's perception of acoustical body sounds and his relation to both disease and patient. Despite the clear superiority of the instrument in sound auscultation, it was accepted with some antagonism even by prominent chest physicians.⁴ The amusing critics included "The stethoscope is largely a decorative instrument. . . Nevertheless, it occupies an important place in the art of medicine. . ." or even complaints of physicians that "they heard too much."

^bThe sleep apnea syndrome represents a complex medical problem characterized by a cessation of effective respiration during sleep. In particular, the so-called obstructive apneas are of great interest, which are characterized by an obstruction of the upper airways and obstructive snoring, i.e. intermittent, loud and irregular snoring. The minimum prevalence of the apneas is about 1%, the apneas causing a severe deterioration of quality of life, excessive daytime somnolence, decreased life expectancy, and negative effects on other family members.^{5,6}

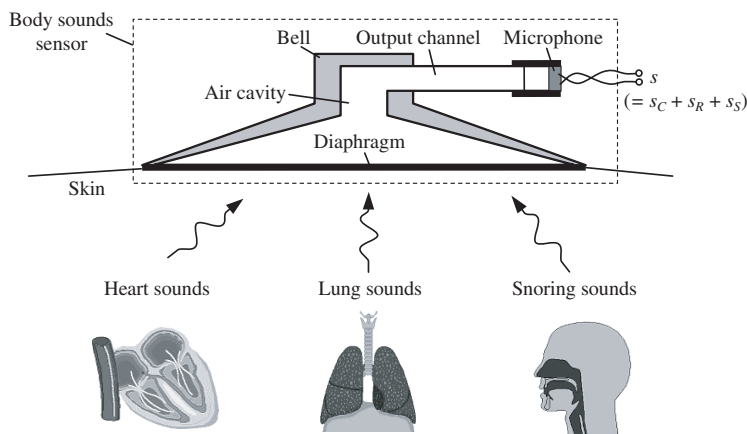


Fig. 1. Recording of the heart, lung, and snoring sounds by means of the body sounds sensor — a microphone attached to a chestpiece (component of the stethoscope) by a plastic tube. The cross section of the chestpiece is shown, which depicts the diaphragm and the bell with its output channel.

- cardiac component s_C ,
- respiratory component s_R , and
- snoring component s_S .

2.1. Heart sounds

The heart sounds are perhaps the most traditional sounds, as indicated by the fact that the stethoscope was primarily devoted to the auscultation of the heart sounds. These sounds are related to the contractile activity of the cardiohemic system^c and particularly yield direct information on myocardial and valvular deterioration or on hemodynamic abnormalities.^{11,12}

The normal and abnormal heart sounds are generated within the heart (Fig. 2) and may include the following sounds,^{11,13–15} as schematically demonstrated in Fig. 3:

- (i) the first sound,
- (ii) the second sound,
- (iii) the third sound,
- (iv) the fourth sound,
- (v) ejection sounds,
- (vi) opening sounds, and
- (vii) murmurs.

^cThe cardiohemic system represents the heart and blood together and may be compared to a fluid-filled balloon, which, when stimulated at any location, vibrates as the whole and thus emits the heart sounds.¹¹

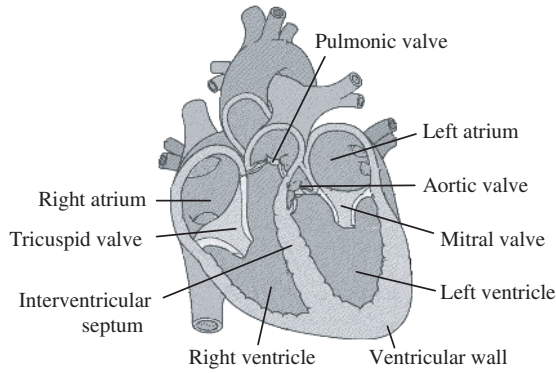


Fig. 2. Heart anatomy relevant for the generation of the heart sounds.

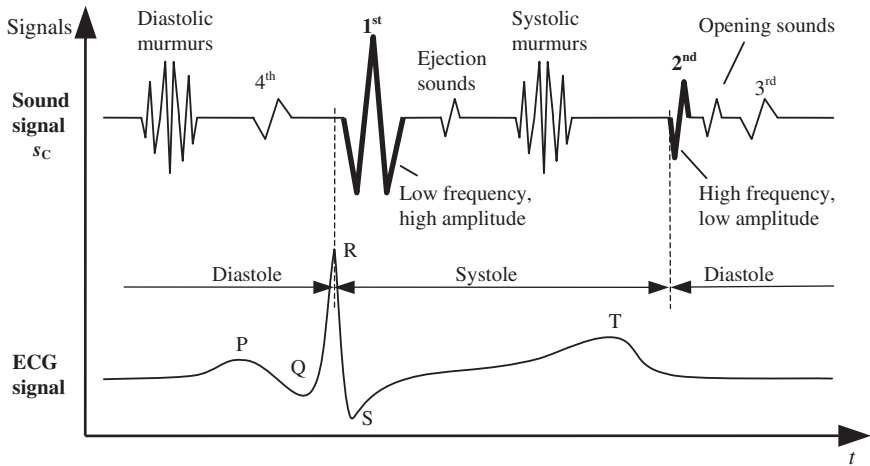


Fig. 3. Schematic representation of the heart sounds in relation to electrocardiogram (ECG) signal with indicated positions of typical waves P, Q, R, S and T. The amplitude and frequency of the sounds are qualitatively indicated, and the normal sounds are drawn in bold.

The first sound: This sound is initiated at the onset of ventricular systole and is related to the close of the atrioventricular valves, i.e. the mitral and the tricuspid valve. Abrupt tension of the valves, deceleration of the blood, and jerky contraction of the ventricular muscles yield vibrations which manifest as the first heart sound. It is the loudest and the longest of all the heart sounds and consists of a series of vibrations of low frequencies. The sound duration is about 140 ms. The frequency spectra of the first heart sound has a peak about 30 Hz with a -18 dB/octave decrease in intensity, whereas the intensity decrease in the range $[10,100]$ Hz is about 40 dB.

The second sound: It is generated by the closure of the semilunar aortic and pulmonic valves when the interventricular pressure begins to fall. Analogous to the

first heart sound, the vibrations occur in the arteries due to deceleration of blood; the ventricles and atria also vibrate due to transmission of vibrations through the blood and the valves. The sound is of shorter duration of about 110 ms (< 140 ms) and lower intensity, and has a more snapping quality than the first heart sound, as will be demonstrated later. The reason for the shorter duration is that the semilunar valves are much tauter than the atrioventricular valves and thus tend to close much more rapidly. As a result of the short duration, the second sound is composed of high frequency vibrations. Contrary to the first heart sound, the second sound does not show any consistent spectral peak, but rolls off more gradually as a function of frequency with an intensity decrease of only 30 dB (< 40 dB) over the range [10,100] Hz.

The third sound: It occurs in early diastole, just after the second heart sound, during the time of rapid ventricular filling when the ventricular wall twitches. The vibrations are of very low frequency because the walls are relaxed. The sound is abnormal if heard in individuals over the age of 40.

The fourth sound: This sound is an abnormal diastolic sound which occurs at the time when the atria contract during the late diastolic filling phase, displacing blood into the distended ventricles. The fourth heart sound is heard just before the first heart sound and is a low frequency sound.

Ejection sounds: They are produced by the opening of the semilunar aortic or pulmonic valves, in particular, when one of these valves is diseased. The sounds arise shortly after the first heart sound with the onset of ventricular ejection. The ejection sounds are high frequency clicky sounds.

Opening sounds: They are most frequently the result of a sudden pathological arrest of the opening of the mitral or tricuspid valve. The sounds occur after the second heart sound in early diastole and represent short high frequency sounds.

Murmurs: These sounds, by definition, are sustained noises that are audible during the time periods of systole (= systolic murmurs) and diastole (= diastolic murmurs). Basically, the murmurs are abnormal sounds and are produced by

- (a) backward regurgitation through a leaking valve,
- (b) forward flow through a narrowed or deformed valve,
- (c) high rate of blood flow (= turbulent flow) through a normal or abnormal valve, and
- (d) vibration of loose structures within the heart.

The systolic and diastolic murmurs consist principally of high frequency components in the range^d [120,600] Hz, occasionally ascending to 1000 Hz.

^dIn particular, the systolic murmurs of aortic insufficiency and the mitral diastolic murmurs fall in the range [20,115] Hz.^{1,2} The aortic diastolic murmurs and pericardial rubs occur at higher frequencies in the range [140,600] Hz. The presystolic murmurs lay, for the most part, in the range below 140 Hz, but may contain components up to 400 Hz.

In normal subjects, only the first and the second heart sound are audible (Fig. 3), as the other sounds are normally of very low intensity. Concerning the spectral region of both normal heart sounds, early studies¹ found that the energy components above 110 Hz are negligible. The main frequency components were found to fall in the approximate range [20,120] Hz.² However, the second heart sound includes more high frequency components than the first sound,¹⁴ which complies with the respective origin of the sounds, as discussed above. Furthermore, the second heart sound is not confined to a narrow frequency bandwidth lacking in concentrated energy which is also contrary to the first heart sound.

Figure 4 demonstrates the normal cardiac sounds for a healthy subject during breath hold, as registered by the body sounds sensor (Fig. 1).⁵ It consists of s_C , which shows cardiac rate f_C close to 0.9 Hz. According to the spectrogram, the first and the second heart sound are mainly characterized by short-term frequency components of up to approximately 100 Hz, with weak harmonics of up to approximately 500 Hz. In the intermediate time intervals, the spectrum is restricted to about 50 Hz. It can be observed that the second heart sound shows slightly higher spectral amplitudes and is shorter in duration ($\Delta t_1 > \Delta t_2$, Fig. 4), which is in full agreement with the discussed behavior of the first and the second heart sound.

Obviously, the frequency components of the heart sounds overlap with those of the breath sounds (Sec. 2.2), especially with the low frequency components of the breath sounds spectrum.¹⁵ The particular interference of the heart sounds in the breathing sounds recorded on the neck was investigated by Lessard and Jones.¹⁴ The authors have shown that the contribution of the heart sounds cannot be neglected even at frequencies above 100 Hz. The first sound was shown to contribute to the acoustic power in the frequency band [75,125] Hz during expiration and to band [175,225] Hz during inspiration. The second heart sound appeared to contribute

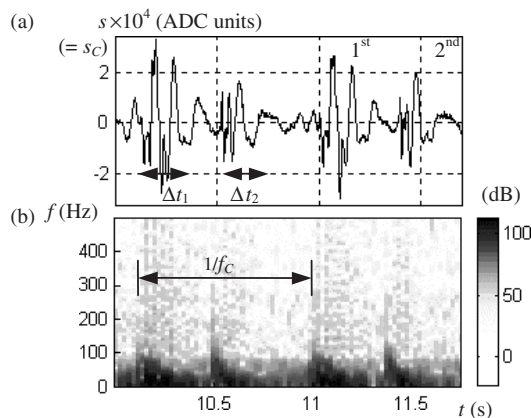


Fig. 4. Heart sounds during breath hold. (a) Sound signal s in the time domain, restricted to the cardiac component s_C including first and second heart sounds. (b) The spectrogram shows higher spectral amplitudes of the second heart sound ($\Delta t_1 > \Delta t_2$).

to the acoustic power in the more extended bands, namely [75,325]Hz during expiration and [75,425]Hz during inspiration. It should be noted that the latter observation is consistent with the aforementioned intensity decreases of the first and the second heart sound.

2.2. Lung sounds

Unlike the heart sounds, the situation with the respiratory induced lung sounds is considerably more complicated, though devaluated by some physicians 30 years ago as “the sound repertoire of a wet sponge such as the lung is limited.”¹⁶ Today, the most promising application areas of the lung sounds are in the upper airway diagnostics, e.g. monitoring of apneas,^b in the lower airway diagnostics, e.g. registration of asthma, and in the registration of regional ventilation.

Generally, the lung sounds are caused by air vibrations within the lung and its airways that are transmitted through the lung tissue (= lung parenchyma) and thoracic wall^e to the recording site.⁴ The lung sounds depend upon several factors, such as airflow, inspiration and expiration phases, site of recording, and degree of voluntary control, and are spread over a wide frequency band,¹⁷ as will be discussed in the following.

The status of the lung sounds nomenclature is best viewed in terms of a historical fact that Laennec, inventor of the stethoscope (refer to footnote a), noted that the lung sounds heard were easier to distinguish than to describe.^f No doubt, high variability of the lung sounds yielded at that time and yields up to now difficulties in the reproducibility of observations. However, the lung sounds can be roughly categorized into

- normal sounds which are characteristic for healthy subjects and
- abnormal sounds heard in pathological cases only.

The most common classification of the normal lung sounds is based on their location, i.e. their auscultation region.^{4,15-19} Three following types of the normal sounds can be distinguished:

- (i) tracheobronchial sounds,
- (ii) vesicular sounds, and
- (iii) bronchovesicular sounds.

^eThe vibration amplitude may be less than $10\ \mu\text{m}$ depending on the method of recording. For instance, mechanical loading by a massive chestpiece (compare Fig. 1) would limit the amplitude of the skin surface motion, for the stress of the skin beneath the chestpiece is increased.

^fTo accommodate the difficulties in describing the lung sounds, familiar sounds (at that time) were chosen to clarify the distinguishing characteristics.⁴ Descriptive and illustrative sounds were used as “crepitation of salts in a heated dish,” “noise emitted by healthy lung when compressed in the hand,” or even “cooing of wood pigeon.”

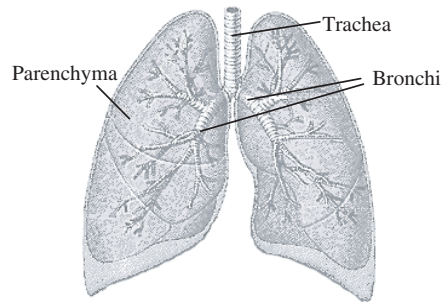


Fig. 5. Lung and adjacent airways relevant for the generation of the lung sounds.

Tracheobronchial sounds: The bronchial and tracheal breath sounds are heard over the large airways (4 mm and larger), e.g. on the lateral neck. The generation region of these sounds is situated centrally and is primarily related to the turbulent airflow in the upper airways, i.e. the trachea and bronchi (Fig. 5). The high air velocity^g and turbulent airflow induce vibrations in the airway gas and airway walls. The vibrations that reach the neck surface are then recorded as the tracheobronchial sounds. These sounds show hollow character, are loud, and contain frequency components up to about 1 kHz, the spectral response curve falling sharply to reach the base line levels in the range [1.2,1.8] kHz.¹⁷ Furthermore, a typical characteristic of these sounds is a silent gap^h between inspiration and expiration.

Vesicular sounds: These sounds are heard on the thorax in the peripheral lung fields through alveolar tissue. They mainly arise due to air movements into the small airways of the lung parenchyma (Fig. 5) during inspiration. The air branches into smaller and smaller airways as it moves to the alveoli, and turbulences are created as the air hits these branches of the airways. These turbulences are suspected of producing the vesicular sounds. Contrary to the inspiration, the air flows during the expiration from small airways to much larger less confining ones and does not contact the airway surfaces. Thus there is much less turbulence created during the expiration and therefore less sound. At the expiration also the tracheobronchial sounds (with their central source) significantly contribute to the relatively weak surface sounds on the thorax. As a result, the sounds during the inspiration are produced in the locally distributed sources in the periphery of the lung and show relatively high amplitudes and high frequency maxima; during the expiration the sounds originate more centrally and are relatively weak because of long transmission paths. The latter behavior is demonstrated in Fig. 6(a) showing that the vesicular sounds, as recorded by the body sounds sensor (Fig. 1), occur mainly during the inspiration. For instance, Fachinger¹⁹ reports that the inspiratory sounds show

^gThe airflow of lower velocity is laminar in type and is therefore silent.

^hThe reason for this gap is that the tracheobronchial sounds come only from the largest airways, the trachea and bronchi, the sounds disappearing temporally at the end of inspiration because at this moment the flow of air passes through the peripheral part of the lung.²⁰

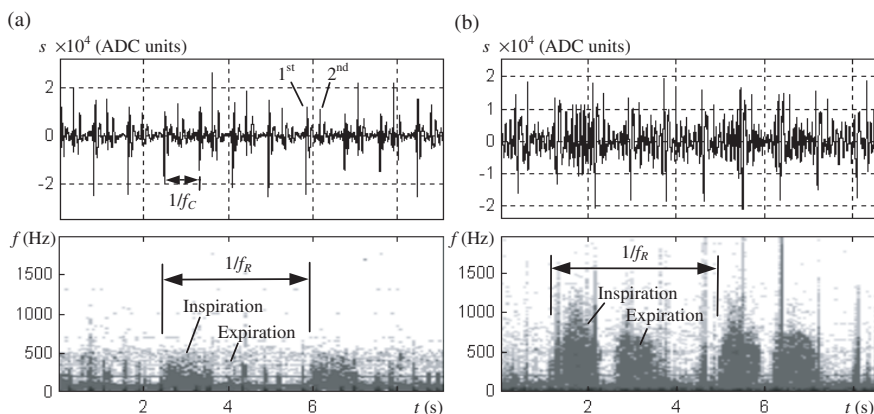


Fig. 6. Lung sounds during normal breathing. (a) Vesicular sounds in the time and spectral domain when recorded on the chest. (b) Tracheobronchial sounds recorded on the neck.

twice as large intensity on the anterior chest as that of the expiratory sounds. Generally, the vesicular sounds are clearly distinguishable at about 100 Hz but the amplitude fall-off to baseline values at about 1 kHz is much more rapid than for the tracheobronchial sounds,¹⁷ as can also be observed in Fig. 6.

Thus, in comparison with the tracheobronchial sounds (Fig. 6(b)), the vesicular sounds (Fig. 6(a)) show lower intensity, smaller spectral range, and more rapid amplitude fall-off with increasing frequency. These differences can be mainly attributed to the fact that the vesicular sounds, when transmitted to the periphery, are filtered to a greater extent than the tracheobronchial sounds. The vesicular sounds have longer transmission paths with more inertial (= damping) components (Sec. 4). For instance,⁴ the normal lung sounds with frequencies higher than 1 kHz were more clearly detected over the trachea than on the chest wall.

Bronchovesicular sounds: These are breath sounds intermediate in characteristics between the tracheobronchial and vesicular sounds.

The abnormal (or adventitious) sounds are heard in pathological cases only and can be classified^{1,4,16,20–23} into

- (i) continuous sounds with a duration of more than 250 ms and
- (ii) discontinuous sounds arising for a time period of less than 20 ms.

Continuous sounds: These sounds show a musical character and exhibit a larger deviation from the Gaussian distribution than the discontinuous sounds. A further subdivision is commonly used:

- (a) **Wheezes:** The generation mechanism appears to involve central and lower airways walls interacting with the gas moving through the airways. In particular, narrowing and constriction of the airways as well as narrowing to the point where opposite walls touch one another cause the wheezes. Wheezes are high frequency, musical noises.

- (b) **Rhonchi:** These sounds are caused by large airways becoming narrowed or constricted, for instance, due to secretions that are moving through the large bronchioles and bronchi. The sounds are sonorous and are like rapidly damped sinusoids of low frequency.
- (c) **Stridors:** These sounds are musical wheezes that suggest obstructed trachea or larynx.

Discontinuous sounds: This type of sounds arises due to explosive reopening of a succession of small airways or fluid-filled alveoli, previously held closed by surface forces during expiration. The abnormal closure is due to an increased lung stiffness or excessive fluid within the airways. On the other hand, bubbling of the air through secretions is also suspected of generating the discontinuous sounds. In both cases a rapid equalization of gas pressures and a release of tissue tensions occur, which cause a sequence of implosive noise-like sounds. A further subdivision is also used:

- (a) **Coarse crackles:** These are low frequency sounds usually indicative of large fluid accumulation in the alveoli.
- (b) **Fine crackles:** They show shorter duration than the coarse crackles and are high frequency sounds.
- (c) **Squawks:** These explosive sounds represent a combination of the wheezes and crackles, which arise from an explosive opening and fluttering of the unstable airways.

Figure 7 shows vesicular sounds during normal breathing with respiratory rate f_R close to 0.2 Hz, the sounds being recorded by the body sounds sensor (Fig. 1).⁵ It can be seen that s in this case (Fig. 7(a)) is similar to s_C in the case of breath holding (Fig. 4(a)), as the signal level of s_R is about 30 dB lower than that of s_C (compare with Fig. 17 in Sec. 5), thus s_R being completely overlaid by s_C . However, during inspiration we recognize that s_R is slightly superimposed on s_C , as demonstrated in the left fragment of the sum signal s (Fig. 7(a)), but not during expiration, as shown in the right fragment. This difference related to the phases of inspiration and expiration is in full agreement with the aforementioned generation mechanisms of the vesicular sounds.

A clear manifestation of the respiratory activity is restricted to the spectrogram, as one can observe in Fig. 7(b). Here, inspiration appears with a basic frequency f_{R1} close to 250 Hz and a second harmonic at 500 Hz, the value of f_{R1} varying between patients. The expiration is characterized by a noise-like spectrum of even lower intensity (about -15 dB) in the range up to about 500 Hz.

From a practical point of view, one of the most important characteristics of the normal lung sounds is that their intensity reflects the strength of the respiratory airflow F . That is, the amplitude and the frequency maxima of the normal lung sounds increase as F rises, particularly during inspiration.¹⁷

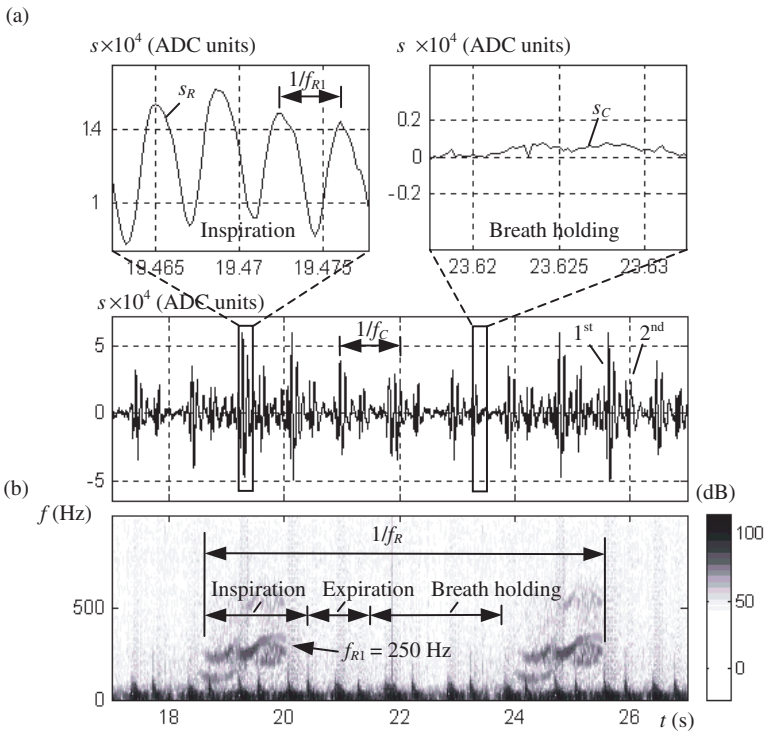


Fig. 7. Vesicular lung sounds during normal breathing. (a) Sensor signal s dominated by s_C (first and second heart sounds). Details are given for the instant of inspiration (left upper figure) and for the break between expiration and next inspiration (right upper figure). (b) The spectrogram with indicated basic oscillation frequency f_{R1} .

For instance, the regional intensity of the vesicular sounds varies with the regional distribution of ventilation,^{4,24} thus the sound intensity is a potentially good measure of regional pulmonary ventilation. The amplitude of s_R could be approximated by an exponential relationship, to give

$$s_R \propto F^n, \tag{1}$$

where n is the power index. The reported values of n were 1.75 and 2 according to Fachinger¹⁹ and Pasterkamp *et al.*,¹⁶ respectively.

Similar to the vesicular sounds, measurements of mean amplitudes and mean frequencies of the tracheobronchial sounds provide a linear measure for F ($n = 1$ in Eq. (1)), in particular, when sounds at higher frequencies are analyzed, e.g. at frequencies above 1 kHz.^{16,25} Dalmay *et al.*¹⁷ confirm this linear relationship, however, for a different frequency range [100,800] Hz. In addition, the latter authors report that the maximum frequency values are shifted upwards as F increases.

It should be noted that the intensity of the lung sounds, especially, of the vesicular sounds and the wheezes, shows a strong inverse relation to the

severity of airflow obstruction.¹⁶ In other words, reduced sound intensity indicates obstructive pulmonary disease while increased intensity is considered indicative of lung expansion.²⁴

The aforementioned high variability of the lung sounds should be addressed in some depth. As shown in many studies,^{16–18,24} sound amplitudes vary greatly from one subject to another, even from sitting to lying position, the variability being more significant during expiration than during inspiration. The variability is mainly due to the strong influence of individual airway anatomy¹⁶ and lung–muscle–fat ratios.¹⁸ An abolishment of this variability was shown to be unsuccessful for identical F or even by an introduction of correction for physical characteristics of subjects, e.g. weight or age of subjects.¹⁷ As a result of the high variability, flagrant disparities can be observed in published quantitative data on the lung sounds.

For instance, the infants exhibit increased vesicular sound intensity and higher median frequency, the differences being attributed, respectively, to acoustic transmission through smaller lungs in combination with thinner chest walls (Sec. 4) and to a different resonance behavior of the smaller thorax.^{16,24} Contrary to the infants and adults, elderly patients show decreased sound intensity due to restricted lung volume, i.e. restricted ventilation. However, the decrease in sound intensity towards higher frequencies is similar at all ages.

The tracheobronchial sounds if heard instead of or in addition to the vesicular sounds almost certainly indicate pathologically consolidated lung.^{4,17,26} This is because the consolidated lung acts like an efficient conducting medium that does not attenuate the transmission of the centrally produced tracheobronchial sounds, as does the inflated normal lung.

2.3. Snoring sounds

Unlike the heart and lung sounds, medical interest has only been recently focused on the snoring sounds. These arise mainly during the inspiration,²⁷ may constitute excessive noise exposure, and may even cause hearing problems.²⁸ Epidemiological studies⁶ have shown that 36% of males and 19% of females were snorers, whereby the prevalence increases significantly after the age of 40, with 50% of elderly population being habitual snorers.²⁹

Generally, the snoring is preceded by a temporal decrease in the diameter of the oropharynx which can be reduced even to a slit, the reduced diameter yielding an increase in the supraglottic resistance.^{27,30} Further narrowing of the oropharynx may lead to not only louder snoring, but also labored breathing. Finally, yet further narrowing can cause complete occlusion of the airways, which manifests as the sleep apnea (refer to Footnote b).

The snoring sounds are mainly generated by high frequency oscillations (= vibrations) of the soft palate and pharyngeal walls, as shown in Fig. 8, as well as by the turbulence of air.^{29,31} Usually the sounds energy is negligible above 2 kHz.³¹

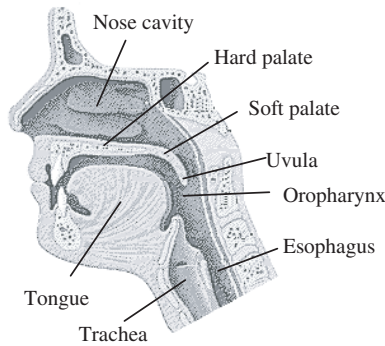


Fig. 8. Pharyngeal airways and surrounding structures relevant for the generation of the snoring sounds.

The rate of appearance of repetitive sound structures during snoring coincides with the time course of airway wall motions and the collapsibility of the upper airways.³² Generally, the characteristics of snoring are determined by the relationship between F and pressure in the upper airways as well as by the airway collapsibility.

Mainly two complementing theories exist, which describe the sound generation mechanisms³¹:

- flutter theory and
- relaxation theory.

The so-called “flutter theory” is devoted to the explanation of the steady continuous forms of the snoring sounds in the time domain. According to this theory, the continuous sounds are produced by the oscillations of the airway walls when the airflow is forced through a collapsible airway and can interact with the elastic walls.

The “relaxation theory” is dedicated to the explosive snoring sounds which are produced by collapsible airways. That is, the low frequency oscillations of the airway walls yield complete or partial occlusion of the lumen with the point of maximum constriction moving upstream along the airway. The repetitive openings of the airway lumen with abrupt pressure equalization generate the explosive sounds.

Similar to the lung sounds (Sec. 2.2), the diversity and the variability of the snoring sounds are extremely large. The snoring sounds may change even from one breath to another. As a result, there is a large number of possibilities to classify the snoring sounds, each of them relying on different bases,

- snoring origination region,
- type of snoring generation, and
- snoring signal waveform.

Obviously, the above classification possibilities are non-exclusive, i.e. some types of the snoring sounds may be described by the use of two or more bases from the above.

Classification based on the snoring origination region,^{27,31} i.e. snoring through

- (i) nose,
- (ii) mouth, or
- (iii) nose and mouth.

Nasal snoring: In this case the soft palate remains in close contact with the back of the tongue, and only the uvula yields high frequency oscillations, the oscillation frequency being about 80 Hz.²⁷ In the frequency domain, the snoring has been demonstrated to show discrete sharp peaks at about 200 Hz, the peaks corresponding to the resonant peaks (= formants) of the resonating cavities of the airways and suggesting a single sound source.³¹

Oral snoring: This type of snoring is characterized by an ample oscillation of the whole soft palate. The oscillation frequency of about 30 Hz²⁷ is lower than that during the nasal snoring because the oscillating mass of the soft palate is larger than that of the uvula.

Oronasal snoring: These snoring sounds include both nasal and oral snoring. The corresponding spectrum shows a mixture of sharp peaks and broad-band white noise in the [400,1300] Hz range.³¹ The large number of peaks may reflect two or more segments oscillating with different frequencies.

Classification according to the type of generation,^{27,29,31,32} i.e.

- (i) normal snoring,
- (ii) obstructive snoring, and
- (iii) simulated snoring.

Normal snoring: It is always preceded by the airflow limitation.^{27,31,32} The narrowing of the pharyngeal diameter is thought to be produced by the negative oropharyngeal pressure generated during the inspiration or sleep-related fallⁱ in the tone of upper airway muscles, which yields a passive collapse of the upper airways. Furthermore, the supraglottic pressure and F show 180° out-of-phase oscillations^j and a relatively small hysteresis.²⁷ The snoring sounds show a regular rattling character³¹ with significant spectral components in the frequency range [100,600] Hz and minor components of up to 1000 Hz.²⁹ The normal snoring most likely pertains to the aforementioned “flutter theory.”

Obstructive snoring: This pathological type of snoring is associated with high frequency oscillations of the soft palate. In particular, a strong narrowing of the

ⁱThe pharyngeal muscle tone can be reduced by not only sleep, but also alcohol, sedatives, or neurological disorders.⁶

^jThe 180° out-of-phase relationship between the supraglottic pressure (= pressure drop across the supralaryngeal airway) and F could be explained by successive partial closings and openings of the pharynx by the soft palate, resulting in opposite changes in the supraglottic pressure and F .²⁷

airways and even their temporal occlusion²⁷ occur due to high compliance of the airway walls.³¹ The hysteresis between the supraglottic pressure and F is much larger than that during the normal snoring. The obstructive snoring sounds are louder than the normal snoring sounds, exhibit fricative and high frequency sounds, and show intermittent and highly variable patterns. They show an irregular white noise with a broad spectral peak of about 450 Hz and another around 1000 Hz. Furthermore, the ratio of cumulative power above 800 Hz to power below 800 Hz is higher for the obstructive snoring when compared to the normal snoring. The obstructive snoring likely pertains to the already described “relaxation theory,” in contrast to the normal snoring.

Simulated snoring: Contrary to the normal and obstructive snoring, the simulated snoring is not preceded by the air flow limitation.²⁷ The narrowing of the pharyngeal diameter could be produced by voluntary active contraction of the pharyngeal muscles. According to Beck *et al.*,²⁹ the simulated snoring could be characterized as complex waveform snoring (see below).

Classification accounting for the distinct signal waveform patterns,²⁹ i.e.

- (i) complex waveform snoring and
- (ii) simple waveform snoring.

Complex waveform snoring: In the time domain, these snores are characterized by repetitive, equally spaced train of structures which start with a large deflection and end up with a decaying amplitude. The sound structures arise with the frequencies in the [60,130] Hz range showing internal oscillations of up to 1000 Hz. In the frequency domain, a comb-line spectrum with multiple peaks can be observed. The complex waveform snoring may result from colliding of the airway walls with an intermittent closure of the lumen.

Simple waveform snoring: Contrary to the complex waveform snoring, the simple waveform snoring shows a nearly sinusoidal waveform of higher frequency with negligible secondary oscillations. Thus the frequency domain exhibits only 1 up to 3 peaks in the [180,300] Hz range, of which the first is the most prominent. This type of snoring results probably from the vibration of the airway walls around a neutral position without actual closure of the lumen.

Figure 9 shows typical experimental results for different types of snoring which were recorded by the body sounds sensor (Fig. 1).⁵ The variability of snoring proved to be very high, with significant changes in the time and frequency domain being possible even from one breath to the next. Nevertheless, there is an evident difference between the normal and obstructive snoring.

As can be seen in Fig. 9(a), the normal snoring is characterized by distinct heart sound peaks, s_S not appearing clearly in the time domain, which is similar to the appearance of the heart and lung sounds (Figs. 4 and 7). However, the snoring becomes evident in the spectrogram. The given case shows a basic harmonic line $f_{R1} \approx 140$ Hz which also clearly appears in the depicted time domain fragment

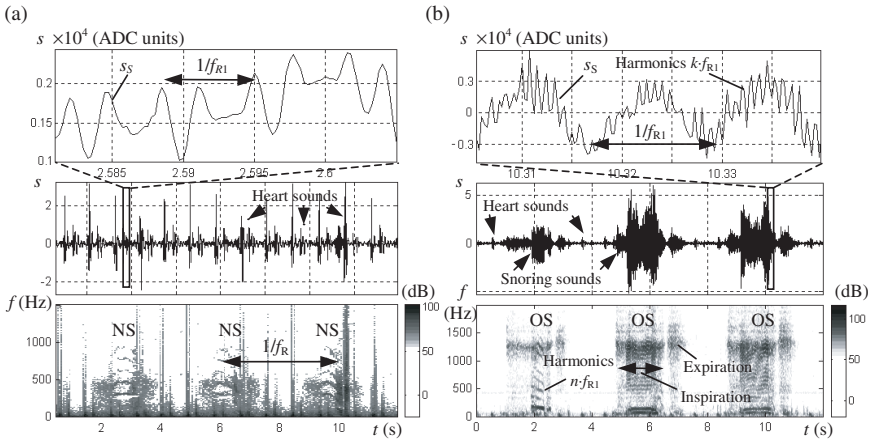


Fig. 9. Snoring sounds including a fragment (upper figure) and the corresponding spectrogram (lower figure). (a) Sensor signal s during normal snoring (NS) from a non-apneic patient, dominated by the heart sounds. (b) Obstructive snoring (OS) dominated by the snoring events from a patient with obstructive sleep apnea.

(upper figure of Fig. 9(a)). Furthermore, we find a series of harmonics up to almost 1000 Hz. This means that compared to the lung sounds during normal breathing, the spectrum proves to be wider here and shows higher intensity, according to the stronger gray tones.

Figure 9(b) shows the obstructive snoring. Contrary to the normal snoring (Fig. 9(a)), the obstructive snoring is not characterized by heart sound peaks in the time domain. Component s_S exhibits much higher amplitudes, the difference being up to approximately 20 dB. The snoring events are also predominant in the spectrogram. Inspiration shows the series of harmonics up to 1000 Hz. It is followed by a noise-like structure which may exceed 1500 Hz and which also appears with lower amplitude during expiration. It can be deduced from the above description that the observed normal snoring (Fig. 9(a)) shows properties of the oronasal and normal snoring, whereas the observed obstructive snoring (Fig. 9(b)) is intermediate in characteristics between oronasal, obstructive, and complex waveform snoring.

A few words should be dedicated to the intensity levels of the snoring sounds, in comparison with the normal lung sounds (Sec. 2.2). Generally, the background noise level in test rooms could reach 50 dB SPL,^k and normal breathing levels could go up to 54 dB SPL.³² The normal breathing levels are in the [40,45] dB SPL range (or [17,26] dBA¹).^{34,35}

^kAbbreviation dB SPL stays for sound pressure measurements in decibels using the reference sound pressure level (SPL) of 20 μ Pa and a flat response network in the frequency domain (compare Footnote 1). For instance, a normal conversation yields about 60 dB SPL, whereas a vacuum cleaner and a pneumatic drill exhibit in a distance of a few meters about 70 dB SPL and 100 dB SPL, respectively.³³

The snoring sound level has spikes in intensity greater than 60 dB SPL^{32,36} or even greater than 68 dB SPL³⁴ and may reach levels of more than 100 dB SPL (according to diverging reports) in a distance of less than 1 m from the head of the patient. According to Schäfer,³⁴ women show reduced snoring sound levels by about 10 dB SPL, whereas Wilson *et al.*²⁸ report about the men–women difference of only about 3 dBA, which translates into a substantially different sound intensity perception. Furthermore, the latter authors report average snoring sound intensities in the [50,70] dBA range of patients with the obstructive snoring, the levels being more than 5 dBA higher for apneic snoring than for non-apneic snoring. An overview³⁵ refers to snoring sound levels up to 80 and 94 dBA for non-apneic snoring and apneic snoring, respectively.

Analogous to the lung sounds (Sec. 2.2), there are reports about the relationship between the snoring sounds and F . As reported by Beck *et al.*,²⁹ the highest and sharpest amplitude deflections of the snoring sounds occur when the amplitude of F is at its highest (compare Eq. (1)).

Similar to the lung sounds, the snoring sounds also show the aforementioned high variability.³⁷ In particular, the variability of the obstructive snoring is very high; the sound characteristics may strongly change even from one breath to the next.²⁹ As suggested by Perez-Padilla *et al.*,³¹ the high variability may arise due to

- (i) changing characteristics of the resonant airway cavities, e.g. pharynx or mouth cavities,
- (ii) variations of the site of collapse of the airway, or
- (iii) varying upper airway resistance since the airways geometry varies from occluded to fully dilated.

It should be noted that the snoring, especially the obstructive snoring, may be related to increased morbidity, systemic hypertension, cerebrovascular diseases, stroke, severe sleep abnormalities, and even impaired cognitive functions.^{6,28,32} As a physiologic example, the duration of the snoring seems to be positively correlated to the strength of oxygen desaturation in blood.³⁸

As already mentioned, there is strong evidence that the obstructive snoring may also be an intermediate in the natural history of sleep apnea syndrome (refer to Footnote b) and thus may be applied for the detection of apneas.^m As shown in Fig. 10, the pathologically narrowed airways can periodically interrupt the snoring by respiratory arrests, followed by sonorous breathing resumptions as apneic gasps

^lAnalogous to the definition of dB SPL (compare Footnote k), abbreviation dBA stays for the sound pressure measurements in decibels, however, employing the A-weighting network that yields the response of the human ear. This network attenuates disproportionately the very low frequencies, e.g. -30 dB SPL at 50 Hz and 0 dB SPL at 1 kHz.³³

^mAn overview of the available literature discloses a number of possibilities for the detection of apneas by the use of the body sounds. In particular, the detection procedures can be roughly classified into three groups, i.e. detection by (i) trained physicians,³⁹ (ii) total sound intensity,^{16,36,38,40–43} and (iii) partial sound intensity within restricted spectral region.^{25,43–48}

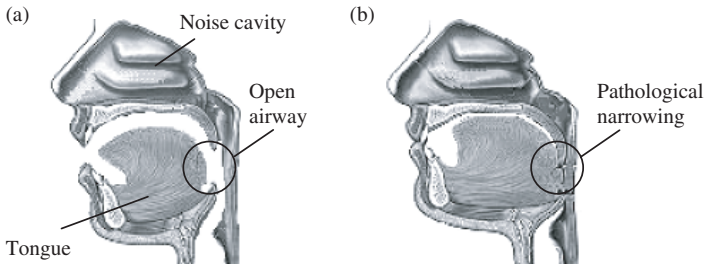


Fig. 10. Pharyngeal airways and surrounding structures (compare Fig. 8) for (a) a non-apneic patient and (b) an apneic patient.

for air.²⁹ Indeed, the snoring is considered as a primary symptom for the sleep apnea⁴¹; however, the snoring is not specific for the apnea.²⁸

Lastly, the physiologic and social factors which favor the snoring should be shortly discussed. Obviously, small pharyngeal area, as demonstrated in Fig. 10, and pharyngeal floppiness (= distensibility), i.e. strong changes in the pharyngeal area in response to externally applied positive pressure, favor the snoring.^{6,41} In addition, cervical position, obesity (= high values of the obesity index, the so-called body mass index BMIⁿ), large neck circumference, presence of space occupying masses impinging on the airway, e.g. soft palate (or uvula) hypertrophy or tumors, and pathological restriction of the nasal airway, e.g. rhinitis, assist the snoring in a disadvantageous way.^{49,50} Among the social factors supporting the occurrence of the snoring, stress, tiredness and alcohol intake are worth to be mentioned. Finally, subjective factors as home environment or sleep lab influence the severity of the snoring, which tends to be higher in the sleep lab.³²

3. Mutual Interrelations of Body Sounds

One can expect that the different body sounds, as described in Secs. 2.1–2.3, are not fully independent, and so the sound components s_C , s_R , and s_S are interdependent. Thus the signal characteristics of the latter components show specific relationships, as schematically demonstrated in Fig. 11, which can be generally attributed to mechanical, neural and functional interrelations between the respective sound generation sources.

We start with the respiratory induced effects on s_C (Sec. 2.1), i.e. with a dependence of s_C on s_R (Fig. 11). During inspiration, these effects can be summarized as follows:

ⁿThe BMI is an anthropometric measure defined as weight in kilograms divided by the square of height in meters. Usually BMI > 30 indicates obesity.

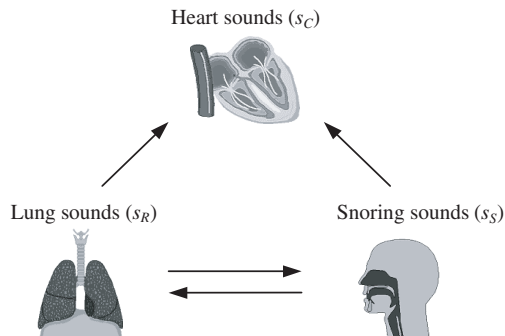


Fig. 11. Mutual interrelations of the different body sounds with indicated direction of influence.

- (i) the second heart sound is split,
- (ii) the right-sided heart sounds are intensified while the left-sided heart sounds are slightly attenuated, and
- (iii) the rate of the heart sounds ($= f_C$) is increased.

The first two effects arise because the heart is in the immediate anatomical vicinity of the lung, which suggests a rather strong mechanical interrelation between the sources of s_C and s_R . Here the source of s_R , in particular, the changing volume of the lung, influences the pressure conditions within the heart and those close to the heart over the respiration cycle. During inspiration, the intrathoracic pressure is decreased, allowing air to enter the lungs, which yields an increase of the right ventricular stroke volume (of the venous blood)^o and a simultaneous decrease of the left ventricular stroke volume (of the arterial blood).^p

The reason for the split heart sound during inspiration (the first effect) can be especially attributed to the temporal increase of the right ventricular stroke volume, which causes the pulmonic valve (Fig. 2) to stay open longer during ventricular systole (Fig. 3). The delayed closure of the pulmonic valve gives rise to a delayed sound contribution to the second heart sound, whereas the preceding contribution

^oIn particular, the right ventricular stroke volume is increased during inspiration because of the respiratory pump mechanism.⁵¹ That is, the intrathoracic pressure decreases, and the pressure gradient between the peripheral venous system and the intrathoracic veins increases.⁵² This causes blood to be drawn from the peripheral veins into the intrathoracic vessels, which increases the right ventricular stroke volume.

^pThe decreased left ventricular stroke volume during inspiration can be mainly attributed to three effects^{51–55}:

- (i) the increased capacity in the pulmonary vessels (see Footnote o) reduces mechanically the left ventricular stroke volume due to leftward displacement of the interventricular septum (Fig. 2),
- (ii) corresponding to the mechanism of the respiratory sinus arrhythmia (see Footnote q), an increase of f_C during inspiration reduces the diastolic filling time of the heart and contributes to the decrease of the left ventricular stroke volume, and
- (iii) the decreased intrathoracic ($=$ pleural) pressure during inspiration lowers the effective left ventricular ejection pressure and impedes the left ventricular stroke volume ($=$ reverse thoracic pump mechanism).

to this sound results from a slightly earlier closure of the aortic valve (Sec. 2.1). In analogy, the earlier closure can be attributed to the decreased left ventricular stroke volume. As a result, the second heart sound is split more strongly during inspiration than during expiration.

The dominance of the right-sided heart sounds during inspiration (the second effect) can be also explained by the increased right ventricular stroke volume. Since these sounds are generated by the closure of the right-sided tricuspid and pulmonic valve (Fig. 2), the increased volume of the decelerated right-sided blood tends to increase the intensity of the right-sided sounds. On the other hand, the amount of blood entering the left-sided chambers of the heart is decreased, which causes the left-sided heart sounds (generated by the closure of the left-sided mitral and aortic valve, Fig. 2) to generally decrease in intensity.

In contrast to the first two effects as discussed above, the third effect is not governed by the mechanical interrelations between the sources of s_C and s_R , but by a neural interrelation in between. Corresponding to the mechanism of the respiratory sinus arrhythmia,⁹ the value of f_C increases temporally during inspiration, whereas the reverse is true for expiration. In addition, the degree of the variation of f_C is also significantly controlled by impulses from the baroreceptors in the aorta and carotid arteries since the blood pressure also changes over the breathing cycle.⁵⁵

Obviously, the mutual interrelation between s_R and s_S is very strong (Fig. 11), for the respective sources are governed by the same breathing activity. This intrinsic dependence yields identical respiratory and snoring rate ($= f_R$); nonetheless, the signal properties of s_R and s_S are very different (Secs. 2.2 and 2.3). In addition, one can also expect an indirect interrelation between s_R and s_S . For instance, the obstructive snoring may intermittently occlude the upper airways, which could temporally alter the resonance characteristics of the upper airways and thus the spectral content of s_R .

At last, the dependence of s_C on s_S will be shortly addressed (Fig. 11). In healthy subjects, this dependence equals the discussed dependence between s_C and s_R , for both s_R and s_S are of the respiratory origin. However, in pathological cases the obstructive snoring may strongly influence s_C since the obstruction overloads the heart, favoring cardiovascular diseases (compare Sec. 2.3). In particular, the influence on s_C gets stronger when the obstructive snoring occurs in combination with the intermittent closures of the airway lumen, i.e. with the intermittent apneas (see Footnote b).

Figure 12 exemplifies the discussed relationship between s_C and s_R , the latter components assessed by the body sounds sensor (Fig. 1). The depicted envelope in Fig. 12(a) demonstrates the intensification of the heart sounds ($= s_C$) during

⁹The respiratory sinus arrhythmia occurs through the influence of breathing on the sympathetic and vagus impulses to the sinoatrial node which initiates the heart beats.^{52,55} During inspiration, the vagus nerve activity is impeded, which increases the force of contraction and raises f_C , whereas during expiration this pattern is reversed.

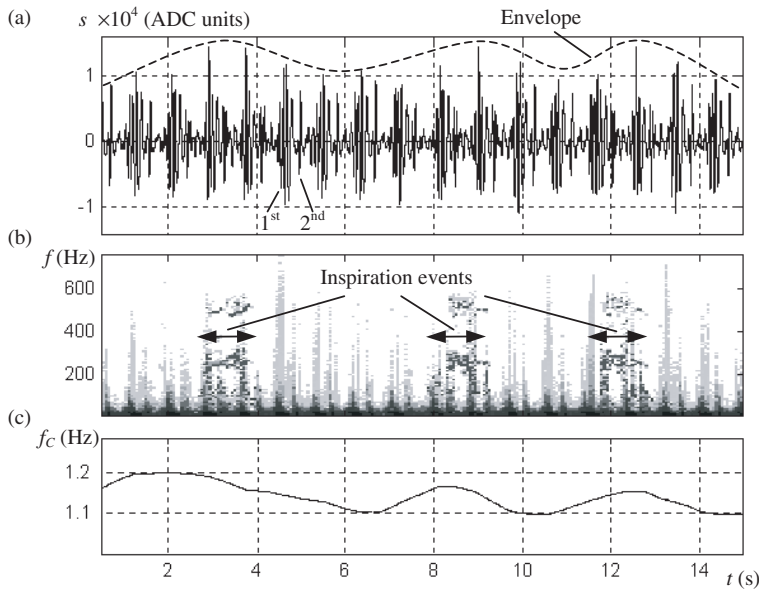


Fig. 12. Mutual dependence of the heart and lung sounds. (a) Sensor signal s with prevailing s_C (first and second heart sounds) and the respiratory induced envelope. (b) The corresponding spectrogram. (c) Variation of the heart rate f_C over respiration cycles.

inspiration, the inspiratory events ($= s_R$) being recognizable in the spectral domain (Fig. 12(b)). Furthermore, Fig. 12(c) shows that the values of f_C increase temporally during the phases of inspiration, which is in full agreement with the aforementioned effect of the respiratory sinus arrhythmia (see Footnote q) on f_C .

It can be deduced from the latter experimental observation that the amplification of the right-sided heart sounds during inspiration is stronger than the concurrent attenuation of the left-sided heart sounds, since the total intensity of the heart sounds raises. In addition, an identical tendency of the amplitude of s_C to increase during inspiration can be observed in Fig. 7(a) which depicts a different experimental data set. However, the observed dominance of the amplification of the right-sided heart sounds versus the non-dominant attenuation of the left-sided heart sounds during inspiration may not be generally valid. This is because there are published data⁵⁶ that demonstrate the opposite behavior, namely the intensity of the heart sounds was observed to increase during expiration.

4. Transmission of Body Sounds

The total acoustical path of the body sounds begins with a vibrating structure which may be given by vibrating valves yielding the heart sounds or air turbulences in the upper airways accounting partially for the lung and snoring sounds (Secs. 2.1–2.3). These mechanically generated vibrations propagate within the body tissues along

many paths toward the skin surface. However, a large percentage of the sound energy never reaches the surface because of spreading, absorption, scattering, reflection, and refraction losses.

Arrived to the skin surface, the body sounds cause skin vibrations of three different waveforms: transversal (or shear) waves, longitudinal (or compression) waves, and a combination of the two.³ The resulting vibrations of the skin serve as a sound source accessible to the body sounds sensor, in particular, to the chestpiece diaphragm (Fig. 1). In addition, viscoelastic properties^f of the skin make the interaction between the sounds and the skin even more complex.

4.1. Propagation of sounds

4.1.1. General issues

The propagation of the body sounds as well as any other acoustic waves in the time and space domain is a subject of the following simple relationship:

$$\lambda = \frac{v}{f}. \quad (2)$$

Here, symbol λ is the sound wavelength, v is the sound velocity, and f is the sound frequency. In particular, the above equation describes the interrelation between the spatial sound characteristic λ and the time-related characteristic f by the use of the time-spatial characteristic v . The value of v is determined through physical properties of the propagation medium, to give

$$v = \sqrt{\frac{\kappa}{\rho}} = \sqrt{\frac{1}{\rho \cdot D}}. \quad (3)$$

Here, κ is the module of the volume elasticity, ρ is the density of the propagating medium, and $D (= 1/\kappa)$ is the compliance or adiabatic compressibility. In the case of gases, e.g. air, κ is expressed as the product of adiabatic coefficient and gas pressure.

Obviously, Eqs. (2) and (3) account for the sound propagation in any type of homogeneous medium, including the biological tissue. Table 1 summarizes the values of v and λ for the most relevant types of biologic media involved in the transmission of the body sounds. One can observe that the lung parenchyma for which ρ and D are given by the mixture of the tissue and the air yields a relatively low v in the order of only 50 m/s (23 m/s up to 60 m/s¹⁸), the value depending strongly on air content.⁵ This value is much lower as compared with v in the tissue (≈ 1500 m/s) or

^fThe viscoelastic material demonstrates both viscous and elastic behavior under applied sound wave pressure which yields internal stress. That is, the material requires a finite time to reach the state of deformation appropriate to the stress and a similar time to regain its unstressed shape. In particular, the viscoelastic material exhibits hysteresis in the stress-strain curve, shows stress relaxation, i.e. step constant strain causes decreasing stress, and shows creeping, i.e. step constant stress causes increasing strain.^{57,58}

Table 1. Approximate values of the sound velocity in air, water, muscle,⁷ large airways, tissue,¹⁸ tallow,⁵⁹ and lung.^{18,26,60} Corresponding wavelengths are calculated according to Eq. (2). Approximate absorption coefficients are given according to the classical absorption theory.^{59,61}

	Sound velocity v (m/s)	Wavelength at 1 kHz λ (m)	Classical absorption coefficient at 1 kHz $\alpha_F + \alpha_T$ (1/m)
Air	340	0.34	10^{-5}
Large airways (diameter > 1 mm)	270	0.27	10^{-5}
Water	1400	1.4	10^{-8}
Tissue (\approx water)	1500	1.5	10^{-8}
Muscle (\approx water)	1560	1.56	10^{-8}
Tallow (\approx fat)	390	0.39	10^{-4}
Lung parenchyma	50	0.05	$> 10^{-5}$

in the large airways (≈ 270 m/s) alone. As a result, the lung parenchyma accounts for the lowest values of λ (≈ 5 cm at 1 kHz) which certainly decrease even more with increasing f (Eq. (2)).

It is worth to discuss shortly the influence of temperature ϑ and humidity on v (and λ , Eq. (2)) from a physiological point of view. It is well known⁷ that v in air tends to increase with increasing ϑ , the increase rate $\Delta v/\Delta\vartheta$ being of about 0.6 m/s per °C. Since inspiration brings cold air (usually room air) with $\vartheta < 37^\circ\text{C}$ into the airways and expiration delivers the warmed air with $\vartheta \approx 37^\circ\text{C}$, the value of v in the large airways decreases and increases, respectively. As a result, v oscillates by a few percents over the breathing cycle. The respiratory induced humidity changes in the large airways can also be expected to influence the effective value of v ; however, the influence is practically negligible. To give an example, a humidity change from 80% during inspiration to 100% during expiration yields an increase in v of only about 0.2% (or 0.7 m/s) at $\vartheta = 37^\circ\text{C}$.

^sThe value of v in the lung parenchyma can be theoretically estimated by Eq. (3) considering air content. If we assume that the volumetric portion of the air is 75% and the rest is the tissue,²⁶ then ρ_L and D_L of the lung (= composite mixture) can be estimated as

$$\rho_L = 0.75 \cdot \rho_A + 0.25 \cdot \rho_T \approx 0.25 \cdot \rho_T$$

and

$$D_L = 0.75 \cdot D_A + 0.25 \cdot D_T \approx 0.75 \cdot D_A,$$

where ρ_A (1.3 kg/m³) and ρ_T (1000 kg/m³) are the densities of the air and tissue, respectively. Correspondingly, D_A (7000 1/GPa) and D_T (0.5 1/GPa) are the compliances of the air and tissue, respectively. Here, the value of D_A was estimated by the use of Eq. (3) with v of the air (Table 1) and ρ_A as parameters. The values of ρ_T and D_T were approximated by the corresponding characteristics of the water, for the tissue consists mainly of water.

As a result, Eq. (3) yields v 28 m/s for the lung parenchyma with ρ_L and D_L from the above, the calculated value fitting well the reported [23,60] m/s range.¹⁸

4.1.2. Spreading of sounds

If the calculated values of λ in Table 1 are put into relation with distance r from the body sound sources (e.g. heart valves or upper airways) to a possible auscultation site on the chest (Fig. 13), then it becomes obvious that primarily the near field condition ($r < 2 \cdot \lambda$) prevails on the auscultation site. That is, the relevant relation $r < 2 \cdot \lambda$ is supported by the scaled real cross-section of the thorax, as shown in Fig. 13(a). It demonstrates that the practically relevant values of r are in the [0.2,0.3]m range. On the other hand, the size of the body sound sources is in the order of λ , which also supports the assumption of the near field.

One would observe that r is smaller or at least equal to λ in all types of the propagating media but not in the lung parenchyma (Table 1). The high frequency body sounds traveling through the parenchyma ($\lambda \approx 2.5$ cm at $f = 2$ kHz) would not meet the near field condition from the above. However, as will be shown in Sec. 4.1.3, the high frequency body sounds tend to take the airway bound route within the airway-branching structure but not the way bound to the inner mediastinum and parenchyma.

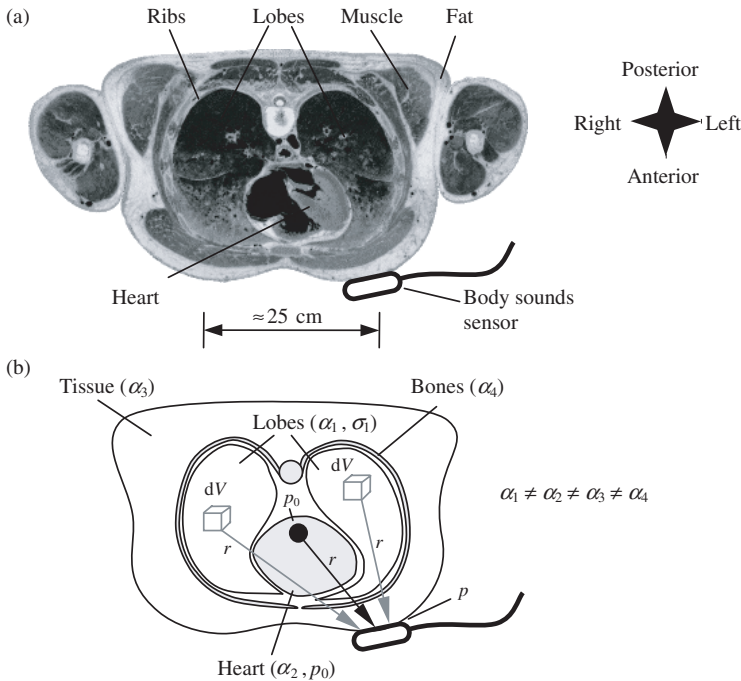


Fig. 13. Propagation of the body sounds in the thorax.⁶² (a) Cross-section of the thorax in the height of the heart showing highly heterogeneous propagation medium. (b) Contribution of the point source of sound (origin sound pressure p_0 , Eq. (4)) and the distributed sources of sound (volume elements dV with the respective volume density σ of the distributed sound pressure, Eqs. (5) and (6)) to the acoustic pressure p at the applied body sounds sensor as a function of the propagation distance r and the attenuation coefficients α .

In order to discuss the propagation phenomena of the body sounds and their absorption from a more theoretical point of view, two types of prevailing sound sources can be assumed:

- (i) point source of sound, as approximately given in the case of the heart sounds (Sec. 2.1), tracheobronchial lung sounds (Sec. 2.2), and snoring sounds (Sec. 2.3); and
- (ii) distributed sources of sound, as given for the vesicular lung sounds (Sec. 2.2).

In the case of the point source of sound, the sound intensity of the radially propagating sound waves will obey the inverse square law^t under free-field conditions, i.e. without reflections or boundaries. This law yields that the sound intensity at $2 \cdot r$ has one-fourth of the original intensity at r , which can be considered as spreading losses. In addition to the latter intensity decrease, the propagation medium absorbs the sound intensity with increasing r in terms of absorption losses (Sec. 4.2).

Given both phenomena from the above and assuming that the sound intensity is proportional to the square^u of the sound wave pressure p , the amplitude of p can be approximated as a function of r according to

$$p(r) = k \cdot \frac{p_0}{r} \cdot e^{-\alpha(r) \cdot r}. \quad (4)$$

Here, k is the constant, p_0 is the sound pressure amplitude of the point source at $r = 0$, and $\alpha(r)$ is the sound absorption coefficient (Sec. 4.2.1) as a function of r . Here, the geometrical damping factor^v $1/r$ comes from the inverse square law and loses its weight with increasing r while the original radial wave mutates into the plain wave.

Whereas Eq. (4) accounts for $p(r)$ from the point source of sound, the aforementioned distributed sources of sound can be considered by a modified version of Eq. (4), to give

$$p(r) = k \cdot \int_V \frac{\sigma(r)}{r} \cdot e^{-\alpha(r) \cdot r} \cdot dV \quad (5)$$

^tThe inverse square law comes from strict geometrical considerations. The sound intensity at any given radius r is the source strength divided by the area of the sphere ($= 4 \cdot \pi \cdot r^2$) which increases proportional to r^2 .⁷

^uThe assumption of the proportionality between the sound intensity ($= p^2/Z$ with Z as the sound radiation impedance) and p^2 is strictly held only under far-field conditions ($r > 2 \cdot \lambda$).

^vGenerally, different assumptions regarding the geometrical damping factor can be found in literature. For instance, the damping factor $1/r$ in Eq. (4) was neglected completely by Wodicka *et al.*,²⁶ i.e. the authors assumed plain wave conditions for the propagation of the sound intensity ($\propto p^2$, compare Footnote u) in the lung parenchyma. On the other hand, the studies by Kompis *et al.*^{18,63} assumed an even stronger geometrical damping factor of $1/r^2$ for the assessment of the spatial distribution of p within the thorax region.

with

$$p_0 = \int_V \sigma(r) \cdot dV. \quad (6)$$

Here, p_0 from Eq. (4) is substituted by $\sigma(r)$ which represents the volume V density of the distributed sound pressure (Eq. (6)).

Figure 13 demonstrates schematically the integration procedure for the highly heterogeneous thorax region (Fig. 13(a)), showing inhomogeneously distributed $\alpha(r)$ (Fig. 13(b)). The point source of sound with p_0 in the heart region and the distributed sources with local sound pressure $\sigma(r) \cdot dV$ in the lung parenchyma contribute to p at the auscultation site, i.e. the application region of the body sounds sensor.

4.1.3. Frequency dependant propagation

The peculiarities of the propagation pathway of the body sounds should be shortly addressed. In particular, the propagation pathway of the lung sounds differs with varying frequency. At relatively low frequencies, i.e. below 300 Hz according to Pasterkamp *et al.*¹⁶ or in the frequency range [100,600] Hz according to Wodicka *et al.*,²⁶ the transmission system of the lung sounds possesses primarily two features:

- (i) The large airway walls vibrate in response to intraluminal sound, allowing sound energy to be coupled directly into the surrounding parenchyma and inner mediastinum via wall motion.
- (ii) The entire air branching networks behave approximately as non-rigid tubes which tend to absorb sound energy and thus to impede the sound traveling further into the branching structure.

As a result of the transmission peculiarities from the above, the propagation pathway at the lower frequencies is primarily bound to the inner mediastinum, the sounds exiting the airways via wall motion. According to Rice,⁶⁰ the lung parenchyma acts nearly as an elastic continuum to audible sounds which travel predominantly through the bulk of the parenchyma but not along the airways.

Contrary to the case of lower frequencies, the airway walls become rigid at the higher frequencies because of their inherent mass, allowing more sound energy to remain within the airway lumen and travel potentially further into the branching structure. Thus, the sounds at the higher frequencies tend to take the airway bound route within the airway-branching structure.

Given the varying pathway of the sound propagation for different frequencies and the dependence of v on the propagation medium (Table 1), it can be deduced that v of the lung sounds at the lower frequencies is lower than v at the higher frequencies. This is because the sounds of the lower frequencies are bound to the parenchymal tissue with $v \approx 50$ m/s and the sounds of the higher frequencies propagate primarily through the airways with $v \approx 270$ m/s. Furthermore, the

varying propagation pathway has strong implications on the asymmetry of the sound transmission, as will be discussed in Sec. 5.

Various experimental data confirm the changing transmission pathway and changing v over the frequency of sounds. For instance, an overview¹⁶ shows that the sound transmission from the trachea to the chest wall occurs with a phase delay of about 2.5 ms at 200 Hz (low frequencies), whereas at 800 Hz (higher frequencies) sound traverses a faster route with a phase delay of only 1.5 ms.^w

Finally, it should be mentioned that an experimental estimation of the transmission characteristics of the sounds can lead even to diagnoses and categorization of diseases, for different diseases affect the transmission in a unique way. For instance, as shown by Iyer *et al.*,²³ this could be achieved in terms of the autoregressive modeling of the lung sounds with the aim to identify one or a combination of the hypothetical sound sources (e.g. random white noise sequence, periodic train of impulses, and impulsive bursts) and to characterize the prevailing sound transmission characteristics.

4.2. Attenuation of sounds

Besides attenuation of the body sounds due to the spreading losses (see geometrical damping factor $1/r$ in Eq. (4)), the ability of sounds to travel through matter depends upon the intrinsic attenuation within the propagation medium. Generally, the attenuation phenomena includes the following effects which will be discussed within the scope of the present chapter:

- (i) volume effects, e.g. absorption and scattering, and
- (ii) inhomogeneity effects, e.g. reflection and refraction.

4.2.1. Volume effects

Obviously, the most important volume effects are the absorption and scattering which account for the loss or transformation of sound energy while passing through a material. The absorption process is represented quantitatively by α in Eq. (4) (compare Fig. 13) and accounts for the influence of all three^{26,59,61,64}:

- (i) inner friction,
- (ii) thermal conduction, and
- (iii) molecular relaxation.

^wThe hypothesis of the parenchymal propagation at the lower frequencies is also supported by the fact that the inhalation of a helium oxygen mixture only weakly affects (= reduces) the phase delay of the sound transmission from the trachea to the chest wall at the lower frequencies.¹⁶ In contrast, the phase delays are significantly reduced at the higher frequencies by the helium oxygen mixture in comparison with the air; a reduction of about 0.7 ms can be observed at 800 Hz with practically no reduction at 200 Hz. Since the inhaled gas mixture shows higher value of v than the air, the above observation proves a more airway bound sound route in the case of the higher frequencies.

The inner friction arises because of the differences in the local sound particle velocities. The friction strength is proportional to the ratio of the dynamic viscosity η to ρ , which shows that the transmission pathways with inertial components yield larger damping. The corresponding friction-related component α_F of α can be calculated as

$$\alpha_F = \frac{8 \cdot \pi^2 \cdot \eta}{3 \cdot \rho \cdot v^3} \cdot f^2. \quad (7)$$

The value of α_F in water is extremely low, e.g. $\alpha_F \approx 10^{-8} \text{ m}^{-1}$ at 1 kHz. The latter value is also approximately applicable to the tissue which consists mainly of water (Table 1). To give an example, the value of p decreases by about 1 dB after 10,000 km sound traveling at 1 kHz in water if only α_F is considered. In the air and large airways α_F increases by a factor of 1000 up to 10^{-5} m^{-1} , which yields a decrease of p by about 1 dB after 5 km sound traveling in air.

The thermal conduction can be interpreted as diffusion of kinetic energy. Since the propagation of the sound wave is linked with the local variations of temperature, the local balancing of these variations by the thermal conduction withdraws the energy from the sound wave. Coefficient α_T accounting for the above energy losses can be calculated as

$$\alpha_T = \left(\frac{c_P}{c_V} - 1 \right) \cdot \frac{2 \cdot \pi^2 \cdot v}{c_P \cdot \rho \cdot v^3} \cdot f^2, \quad (8)$$

where c_P and c_V are the specific heat capacities at constant pressure and volume, respectively, and v is the heat conductivity. In water, the value of α_T is lower than α_F by a factor of 1000, whereas in air α_T is in some order as α_F .

The molecular relaxation contributes also to the acoustic absorption in the tissue. This phenomenon is based on the fact that the rapidly submitted energy from the sound field is primarily stored as rotational energy of atoms of involved molecules and, on the other hand, as translational energy which is proportional to gas pressure. In contrast to the above energies, the vibrations of the molecules themselves start with some delay at the expense of rotational and translational energies. Thus a thermal equilibrium arises with a time constant τ (= relaxation time) between these three types of energies. However, the delayed setting of this equilibrium yields energy losses, accounted by the absorption coefficient α_M ,

$$\alpha_M = \left(1 - \frac{v_0^2}{v_\infty^2} \right) \cdot \frac{2 \cdot \pi^2 \cdot \tau}{v \cdot (1 + (f/f_M)^2)} \cdot f^2. \quad (9)$$

Here, f_M ($= 1/(2 \cdot \pi \cdot \tau)$) is the molecular relaxation frequency determined by the molecular properties, and v_0 and v_∞ ($> v_0^x$) are the sound velocities before

*The value of v_0 is lower than v_∞ because the compressibility at lower frequencies before the relaxation ($f \ll f_M$) is higher than that at higher frequencies ($f \gg f_M$); compare the influence of D on v in Eq. (3).⁶¹

relaxation ($f \ll f_M$) and after relaxation ($f \gg f_M$), respectively. In particular, the energy losses show a maximum at $f = f_M$ concerning the product $\alpha_M \cdot \lambda$. In water, f_M shows a very high value of about 100 GHz. This high value of f_M ($\gg 2$ kHz) induces a very small α_M of about 10^{-8} m^{-1} and a strong frequency dependence of α_M ($\propto f^2$) in the frequency range of the body sounds (Sec. 2). In water, the resulting value of α_M is in the range of α_F . Contrary to the case of water, the value of f_M in air is in the human acoustic range, the relaxation induced mainly by oxygen molecules ($f_M \approx 10$ Hz) and water molecules, the content of which is given by the air humidity. Thus α_M in air is relatively large and amounts to about 10^{-3} m^{-1} at 1 kHz.

It is important to observe from Eqs. (7) and (8) that the sound absorption increases with increasing f , in particular, α_F and α_T are proportional to f^2 . The total absorption α , as used in Eq. (4), can be given as the sum of the discussed absorption coefficients, to give

$$\alpha = \alpha_F + \alpha_T + \alpha_M. \quad (10)$$

Table 1 compares α_F and α_T for the relevant types of biologic media involved in the sound transmission. It can be observed that the adipose tissue is the strongest absorber, followed by the air and airways, if only the inner friction and thermal conduction are considered. However, it should be stressed that α_F and α_T represent only the lowest threshold of the real absorption coefficient,^y the component α_M in Eq. (10) being usually larger than the sum $\alpha_F + \alpha_T$ by a few orders of magnitude.

The scattering is the second volume effect being relevant for the attenuation of the propagating body sounds. Generally, the sound energy is scattered, i.e. redirected in random directions, when the sound wave encounters small particles.^z If the size of particles is much smaller^{aa} than λ , then the Rayleigh scattering occurs, whereas for larger particles the Mie scattering is the relevant phenomenon.^{bb} Since the dimensions of the inner body structures, e.g. heart, lung lobes, and bones (Fig. 13(b)), are in the same order as λ (Table 1), the scattering can be expected — from a qualitative point of view — to contribute significantly to the attenuation of the propagating body sounds. Furthermore, it is important to note that the scattering can be quantitatively assessed by a scattering coefficient which is defined in a similar way as α in Eq. (4).

^yFor instance, the absorption in gases is well accounted by the inner friction, thermal conduction, and molecular relaxation. That is, the observed absorption is only slightly higher than the predicted one. However, the real absorption in water is much higher than would be expected on these grounds. The excess absorption can be explained as due to a structural relaxation and a change in the molecular arrangement during the passage of the wave.⁶⁵

^zGenerally, the scattering of acoustic waves in the tissue is due to the chaotic variation in the refractive index at macroscopic scale resulting in dispersion of the acoustic waves in all directions.

^{aa}The scattering of sound waves around small obstacles (dimensions $\leq \lambda$) is also coined as wave diffraction.

^{bb}The Rayleigh scattering presents isotropic scattering (scatters in all directions), while the Mie scattering is of anisotropic nature (forward directed within small angles of the beam axis).

If we consider the volume effects (absorption and scattering) from a more practical point of view, the following observations can be made. An early paper¹ suggests that if the effects of the inner friction ($\approx \eta$, Eq. (7)) are small, as in the case with water, air, and bone, the sound energy may be transmitted with remarkably little loss. In other media, such as fatty breast tissue, the sound waves are almost immediately suppressed (compare Table 1). The flesh of the chest acts also as a significant damping medium since the obesity might completely mask the low frequency heart sounds,¹ as will be demonstrated by own experimental data at the end of this chapter.

Regarding the mentioned theoretical frequency dependence of α ($\propto f^2$), it must be noted that experimental data for the biological tissue suggest a slightly different frequency dependence. That is, Erikson *et al.*⁶⁴ report that α is approximately proportional to f , whereas individual tissues may vary somewhat in between, e.g. hemoglobin has α proportional to $f^{1.3}$. In addition, there are publications^{4,15} which report that the energy of the vesicular sounds (Sec. 2.2) declines exponentially with increasing f , which would imply the proportionality between α and f either.

The obvious consequence of the frequency dependence of α is that the transmission efficiency of the lung parenchyma and the chest wall deteriorates with increasing f , i.e. the tissues act as a lowpass filter which transmit sounds mainly at low f .^{26,66,67} For instance, a model-based estimation of the acoustic transmission has shown a sound attenuation in the [0.5,1] dB/cm range at 400 Hz,¹⁸ the attenuation being negligible at 100 Hz and increasing to approximately 3 dB/cm at 600 Hz.²⁶ It can be derived from the preceding data that α is about 10 m^{-1} according to Eq. (4). That is, the estimated α is higher than $\alpha_F + \alpha_T$ of the tissue according to Table 1 by orders of magnitude, which confirms that α_F and α_T represent only the lowest theoretical threshold of α .

Because of the frequency dependence of α the higher frequency sounds do not spread as diffusely or retain as much amplitude across the chest wall as do lower frequencies. The high frequency sounds are thus more regionally restricted and play an important role in localizing, for instance, the breath sounds to underlying pathology.^{cc}

The non-continuous porous structure^{dd} of the lung parenchyma is of special importance regarding the frequency dependence of the sound absorption. As already

^{cc}For instance, pathologically consolidated lung tissue yields a reduction of the attenuation of the high frequency components and thus a higher amount of high pitched sounds. This is because the intrinsic lowpass filtering characteristics of the lung are pathologically altered, which yields a decrease of the corresponding cut-off frequency. This behavior offers the ability to localize the regions of consolidated lung tissue, and it is the high frequencies of the lung sounds (Sec. 2.2) that facilitate this. To give another example of application, the non-linear spectral characteristics of the sound transmission help to localize also the cardiovascular sounds (Sec. 2.1) to their points of origin.

^{dd}Homogenous materials tend to absorb the acoustic energy mainly because of the inner friction, i.e. due to inner local deformations of the material. Contrary to the homogenous materials, porous materials as the lung parenchyma tend to absorb the acoustic energy also in terms of outer friction, i.e. the friction between the oscillating air particles and porous elements of the material.⁷

mentioned in Sec. 4.1.1, the parenchyma is dominated by the components of tissue and air.^{16,18} That is, the alveoli in the parenchyma act as elastic bubbles in water, whose dynamic deformation due to oscillating p dissipates the sound energy.⁶¹ As long as λ (Table 1) is significantly greater than the alveolar size (diameter < 1 mm), the losses are relatively low. In this case, the losses due to the thermal conduction are considerably larger^{ee} in magnitude than those associated with the inner friction and scattering effects.²⁶ If the value of λ approaches the alveolar size, i.e. f is increasing (Eq. (2)), the absorption exhibits very high losses.¹⁶ However, it is important to note that the spectral range up to 2 kHz, i.e. the relevant spectral range of the body sounds (Sec. 2), yields values of λ which are still significantly larger than the alveolar diameter. For instance, the alveolar size of λ in the lung parenchyma is approached earliest at $f \approx 23$ kHz with $v = 23$ m/s from Sec. 4.1.1.

Indeed, own experimental data gained with the body sounds sensor (Fig. 1) support the findings from the above that the attenuation of the body sounds is significantly influenced by the volume effects. That is, the chest acts as a significant damping medium, and the obesity tends to attenuate significantly the investigated heart sounds (Sec. 2.1). Figure 14 shows a regression analysis for the heart sounds, i.e. the regression between the amplitude of s_C and BMI (see Footnote n). Data of 20 patients were analyzed; in total nine patients had apnea (see Footnote b). It can be deduced from the regression that increasing BMI is linked to the decreasing amplitude of s_C , an increase from 24 to 38 kg/m² causing about 60% loss of the amplitude, the cross-correlation coefficient being about -0.6 . This might indicate that the increasing thickness of tissue and increasing amount of adipose tissue (in patients with higher BMI) yield a strong damping of s_C .

Furthermore, the regression lines in Fig. 14 indicate that the amplitude of s_C is slightly higher for the non-apnea patients in comparison with the apnea patients. This is in full agreement with the clinical signs of apnea, including the risk of apnea

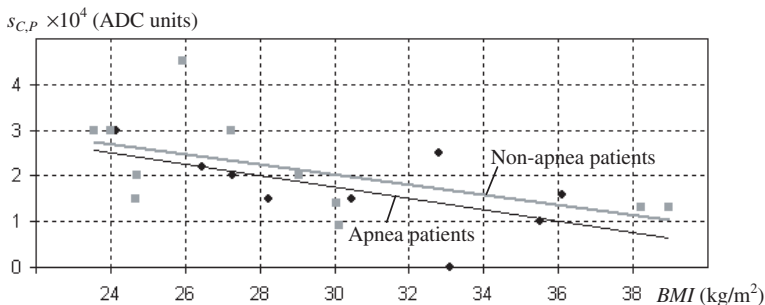


Fig. 14. Relationship between the peak amplitude $s_{C,P}$ of the cardiac component s_C and the body mass index BMI for apnea patients (black) and non-apnea patients (gray), including corresponding linear regression lines.

^{ee}This relation was shown by modeling the lung parenchyma as air bubbles in water, the bubbles being compressed and expanded by the acoustic wave.²⁶

that is strongly interrelated with the increased values of BMI and thus the decreased values of s_C .

Finally, it should be noted that a significant variability of the amplitude of s_C was observed among patients (Fig. 14) but not over the recording time of a single patient. A relatively small amplitude variation of up to 40% over the recording time was mainly caused by the respiratory dependence of the cardiac activity (compare Fig. 12(a)). Contrary to the variability of s_C , the amplitude variability of s_R and s_S (Secs. 2.2 and 2.3) was considerably high among patients as well as over the recording time. This is due to the fact that both s_R and s_S are directly influenced by highly varying strength and type of the respiration among patients as well as over the recording time.

4.2.2. Inhomogeneity effects

The inhomogeneity effects, namely the reflection and refraction, also play an important role within the scope of the body sound attenuation. The spatial heterogeneity of the thorax that reflects the underlying anatomy, as demonstrated in Fig. 13(a), indicates the relevance of the intrathoracic sonic reflections and refractions. In addition, the tubelike resonances^{ff} of the respiratory tract influence the attenuation of the body sounds.¹⁶

The reflection phenomenon describes the relationship between the reflected and incident waves. If the reflection of the inner body sounds is considered on the skin (simplified tissue-air interface), as shown in Fig. 15, then the reflection law yields the following: the reflection angle to the normal matches the incident angle β_T to the normal, and the reflection coefficient R , i.e. the ratio of the reflected and incident p in the tissue, can be given as

$$R = \frac{Z_A - Z_T}{Z_A + Z_T}. \quad (11)$$

Here, Z_A and Z_T are the sound radiation impedances ($= \rho \cdot v$) of air and tissue, respectively. The calculation yields $Z_A \approx 340 \text{ kg m}^{-2} \text{ s}^{-1}$ and $Z_T \approx 1.4 \times 10^6 \text{ kg m}^{-2} \text{ s}^{-1}$, whereas the physical properties of the tissue were approximated by those of water. Given the values from the above, Eq. (11) yields $R \approx -0.998$. This very high value of R indicates that more than 99% of the incident p is reflected and less than 1% is transmitted through the skin if the simplified tissue-air interface is assumed.

^{ff}The tubelike resonances can be attributed to the phenomenon of standing waves within the respiratory tract, which, in approximation, resembles a tube. For instance, the standing waves occur when the open tube length l matches half-wavelength $\lambda/2$ of the acoustic wave passing through it, for the acoustic pressure nodes arise at both open ends of the tube. The resulting harmonic eigenfrequencies f_n

$$f_n = \frac{v}{\lambda} \cdot n = \frac{v}{2 \cdot l} \cdot n$$

with $n (= 1,2,3,\dots)$ as the ordinal number of eigenoscillation provide frequencies at which the transmission efficiency reaches its maximum (compare Eq. (2)).

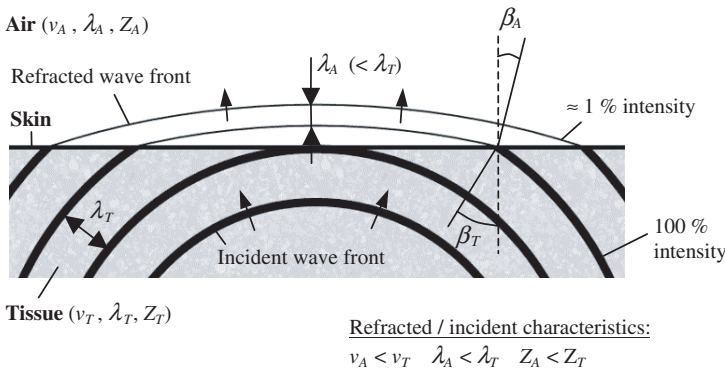


Fig. 15. Reflection losses and refraction of the body sounds when leaving the tissue. The decreasing thickness of the propagating wave front indicates the decreasing intensity due to the reflection losses.

A few restrictions should be mentioned regarding the above estimation of the reflection (and transmission). The first restriction is that the human skin is a true multilayer consisting approximately of three layers: the inmost subcutaneous fat tissue, followed by the dermis, and the outer epidermis. Actually, the transmission of the body sounds through this multilayer would tend to yield a higher transmission rate compared with the simplified tissue–air interface. It is because of the assumption that the respective two neighboring layers would show a less difference in their sound radiation impedances Z_2 and Z_1 than the difference between Z_A and Z_T . As a result, term $|Z_2 - Z_1|$ from Eq. (11) would exhibit a lower value than term $|Z_A - Z_T|$, which would yield a lower R for the respective neighboring layers and thus a higher total transmission rate.

The second restriction is that the reflection law holds only when λ of the sound is small compared to the dimensions of the reflecting surface; otherwise the scattering laws (Sec. 4.2.1) govern the reflection phenomena. Indeed, in the case of the body sounds, the application of the reflection law is limited, since λ (Table 1) and the dimensions of the reflecting surface (Fig. 13) are in the same order. In spite of the above restrictions, the estimated low transmission efficiency ($< 1\%$) underlines the importance of an optimal sound auscultation region, as will be discussed in Sec. 5.

The second inhomogeneity effect is the refraction which describes the bending of acoustic waves when they enter a medium where their v is different. Given the aforementioned simplified tissue–air interface, as demonstrated in Fig. 15, the refracted angle β_A to the normal and β_T obey the Snell's refraction law

$$\frac{v_A}{v_T} = \frac{\sin(\beta_A)}{\sin(\beta_T)}, \quad (12)$$

where v_A and v_T are the sound velocities in air and tissue, respectively. Given the values from Table 1, it can be deduced that $\beta_A < \beta_T$. This means that the refracted wave front of the body sounds is bent toward the normal of the skin, which yields

a more flat wave front in air than in the tissue (Fig. 15). From a practical point of view, the flattened wave front in air favors the sounds auscultation, for the wave front is bunched and redirected toward the body sounds sensor on the skin (Fig. 1). Lastly, it should be mentioned that the discussed restrictions pertaining to the reflection also apply to the refraction phenomenon.

4.3. Coupling of sounds

In addition to the discussed effects of the sound attenuation within the body (Sec. 4.2), the coupling of the body sounds by the body sounds sensor (Fig. 1) should be addressed, since it can be expected to affect the sound attenuation or the gain of p at the microphone diaphragm. As demonstrated in Fig. 16(a), the coupling of the sounds through numerous interfaces within the body sounds sensor, namely from the skin into the chestpiece diaphragm, from the diaphragm into the air within the bell, and finally from the air into the microphone diaphragm, contributes to the sound attenuation.

From a technical point of view, the mechanical/acoustical impedance mismatch in the above interfaces of the sensor accounts for the sound attenuation, for matched impedances would not yield any sound attenuation due to coupling (compare Eq. (11) with $Z_A = Z_T$). The issue of the impedance mismatch can be qualitatively addressed by the use of the electromechanic analogy^{eg} of the resulting skin–diaphragm–air–diaphragm interface, as shown in Fig. 16(b).

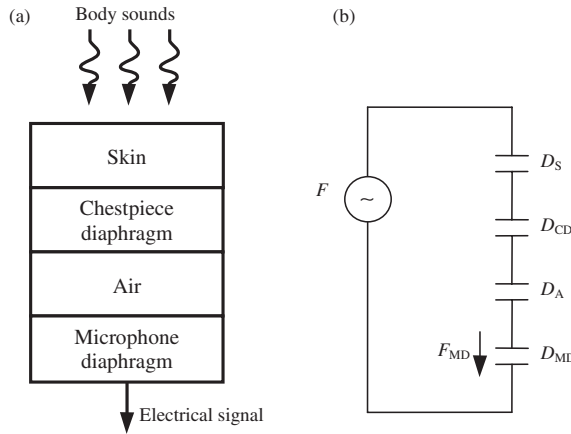


Fig. 16. Coupling of the body sounds by the body sounds sensor (Fig. 1). (a) Sound coupling from the skin, through the chestpiece diaphragm, the air in the cavity of the bell into the microphone diaphragm. (b) Corresponding first electromechanic analogy.

^{eg}Formally, the first electromechanic analogy is used here, which sets the mechanical force analogous to electrical voltage, the sound particle velocity to electrical current, the mechanical compliance to electrical capacity, the mass to electrical inductivity, and the frictional resistance to electrical resistance.⁷ In addition, the first analogy yields electrical circuits which are reciprocally equivalent to mechanical circuits.

For the sake of simplicity, only compliances D of the involved materials are considered here, not accounting for the mass and frictional resistance. It is important to note that the compliances (= feathers) are approximately connected in parallel in terms of mechanical connections because the feathers work against the same sensor housing which is not involved in the oscillations of p . Given the first electromechanic analogy implying a reciprocal electrical circuit, a series connection of the involved D as capacitors results as a model for the sound coupling, as shown in Fig. 16(b). Here, index S of D denotes the skin, index CD stays for the chestpiece diaphragm, index A for the air in the bell, and index MD for the microphone diaphragm.

The interesting quantity within this theoretical investigation is the resulting force F_{MD} on the microphone diaphragm. It represents p acting on the diaphragm and thus accounts for the output voltage of the microphone^{hh} and the output signal s of the body sounds sensor (Fig. 1). According to Fig. 16(b), the value of F_{MD} (or in analogy, the voltage on the capacitor with value D_{MD}) can be then approximated as

$$F_{MD} = F \cdot \frac{D_S \parallel D_{CD} \parallel D_A}{D_S \parallel D_{CD} \parallel D_A + D_{MD}}. \quad (13)$$

Here, F is the total force pertinent to the body sounds entering the skin, and operator \parallel denotes the relevant calculation rule for the series connection of the capacitors. Expression $D_S \parallel D_{CD} \parallel D_A$ indicates the total capacity of the series connection of the capacitors with values D_S , D_{CD} , and D_A . In analogy with the mechanical circuit, term $D_S \parallel D_{CD} \parallel D_A$ represents the total compressibility of all three: the skin, the chestpiece diaphragm, and the air.

It is obvious that the material of both diaphragms is less compressible than the tissue of the skin, whereas the skin is less compressible than the air. As a rough estimation, the diaphragm material can be approximated by acrylic glass (= plexiglass) and the skin tissue by water. Then the following compliance values result: $D_{CD} = D_{MD} = 0.3$ 1/GPa, $D_S = 0.5$ 1/GPa, and $D_A = 7000$ 1/GPa (see Footnote s). With the obvious relation $D_A \gg (D_{CD}, D_{MD}, D_S)$ and the above-mentioned values, the value of F_{MD} can be estimated as

$$F_{MD} \approx F \cdot \frac{D_S \parallel D_{CD}}{D_S \parallel D_{CD} + D_{MD}} \approx F \cdot 0.4. \quad (14)$$

^{hh}The used microphone within the body sounds sensor (Fig. 1) is an electroacoustic transducer (the Sell capacitor⁷) which converts the pressure p variations at its diaphragm into an electrical sensor signal s . The microphone comprises a metallic diaphragm as a first electrode, spaced at a very short distance from a parallel fixed plate which acts as a second electrode. Both electrodes operate as a capacitor which is charged through the charging potential provoked by the permanent polarizing dielectric material in between the electrodes. The variations of p at the microphone diaphragm yield its excursions, which change the capacity in between the electrodes and thus the voltage across the electrodes. As a result, a current through the capacitor is induced, which yields an output voltage (= s) on an external resistor.

The above equation shows that about 40% of the acoustical forces pertinent to the body sounds entering the skin are transmitted to the microphone diaphragm if only the coupling losses are roughly considered. However, this theoretical estimation yields a rather maximum value of the transmission efficiency since neither frictional resistance nor mass was considered.

In addition, the discussed electromechanic analogy allows an important insight into the phenomena of sound coupling. That is, the sound transmission from a medium of low compressibility, e.g. skin, into a medium with high compressibility, e.g. air, is always connected with relatively high losses, whereas the reverse transmission path would show relatively low losses (compare Eq. (13)).

Analogous to the impedance mismatch within the investigated skin–diaphragm–air–diaphragm interface of the body sounds sensor, the impedance mismatch between the different body tissues can be expected to contribute to the attenuation of the body sounds. For instance, Pasterkamp *et al.*¹⁶ report that the impedance mismatch between the parenchyma and the chest wall can account for an order of magnitude decrease in the amplitude of p . This is because the chest wall is significantly more massive and stiff than the parenchyma, although the chest wall is relatively thin.

5. Spatial Distribution of Body Sounds

One would expect from Fig. 13 that the spatial distribution of the hypothetical sound sources inside the body as well as the regional distribution of the surface sounds on the body skin is highly non-uniform. This is because

- sound generation mechanisms lack spatial symmetry with respect to the body axis (Sec. 2) and
- spatial transmission pathways from the sound sources to the skin surface are highly inhomogeneous in terms of acoustic transmission properties (Sec. 4).

The spatial asymmetry of the sound generation mechanisms is primarily given by the massive mediastinum on the left site of the thorax (compare Fig. 13(a)). On the other hand, the inhomogeneous pathways of the sound propagation are caused by the heterogeneous thorax including a mixture of tissue, lung parenchyma, blood, air, and bones (Table 1).

The spatial distribution of the heart sounds was investigated by Kompis *et al.*⁶³ The authors demonstrated that the estimated (= hypothetical) sound sources of the first heart sound are spatially constricted at the expected location of the heart itself. In contrast to the first heart sound, the second heart sound gives rise to more complicated patterns of the sound sources which show multiple spatially separated centers close to the heart region.

Indeed, given the generation mechanisms of the heart sounds (Sec. 2.1), the estimated location of the sound sources pertaining to the first heart sound may be

expected to remain locally constricted to the heart region. In particular, this could be explained by the location of the sound-generating atrioventricular valves which are situated inside of the heart and thus are relatively isolated from outside (Fig. 2). On the other hand, the reported observation regarding the sources of the second heart sound could be explained by the distal location of the semilunar valves, i.e. their distal location with respect to the heart itself. These valves act as output valves whose closures induce vibrations of the external non-constricted blood and tissues, which, in turn, may result in the multiple scattered sound sources in the immediate vicinity of the heart.

The distribution of the hypothetical sound sources of the vesicular lung sounds is consistent with the origin of these sounds (Sec. 2.2), as proven by many authors.^{4,18,19,63,68} Specifically, the estimated distribution supports the concept that the inspiratory sounds are predominantly produced in the periphery of the lung (= distal airways) by distributed sound sources while the expiratory sounds are generated by a more central source in the upper proximal airways.

An important issue is that the transmission of the vesicular lung sounds was shown to be asymmetric, as reported in many papers.^{16,19,24,68} In particular, the sound intensity lateralizes with right-over-left dominance at the anterior upper chest and with left-over-right dominance at the posterior upper chest. The lateralization is followed more closely during expiration and for the lower frequencies (below 300 Hz¹⁶ or 600 Hz²⁶). In addition, anterior sites show a higher sound intensity than posterior sites. It is likely that the observed asymmetries are related to the effects of

- (i) localization of the cardiovascular structures on the left side of the major airways and
- (ii) unsymmetrical geometry of airways.

The preferential coupling of the vesicular sounds to the right anterior chest, especially at the lower frequencies, could be explained by the massive mediastinum on the left side, for the mediastinum may attenuate the sound coupling to the left anterior lung (and the left anterior chest). The effect of the unsymmetrical airways could be pointed out by the fact that the major left segmental bronchi are directed more posteriorly compared with the right bronchi, because of the anterior position of the heart on the left side. Obviously, this asymmetric setting of the bronchi favors the left-over-right dominance of the sound intensity at the posterior upper chest.

The influence of the frequency on the asymmetric sound propagation should be briefly commented. The strong asymmetry which arises for the lower frequencies only can be explained by the frequency dependant propagation of the body sounds. That is, the low frequency sounds are preferentially bound to the lung parenchyma and inner mediastinum, as discussed in Sec. 4.1.3. As a result, the asymmetrical localization of inner body structures plays an important role only

at the lower frequencies. At the higher frequencies, the asymmetry of the sound transmission is weaker because the sound pathway changes to a predominantly airway bound route and is more direct and symmetric, bypassing the effect of the mediastinum.

The regional distribution of the snoring sounds on the skin surface could be approximately derived from the lateralization of passively transmitted sounds introduced at the mouth. These artificially introduced sounds could be roughly equated with the snoring sounds which originate close to the mouth, i.e. in the pharyngeal airway (Sec. 2.3). Given the above assumption and using the data⁶⁸ of the passively transmitted sounds, it can be expected that the snoring sounds would lateralize with right-over-left dominance at the anterior upper chest. At the posterior chest, the snoring sounds should be slightly louder on the left side. In addition, anterior sites would be expected to show a higher snoring sound intensity than posterior sites.

The regional distributions of the sound intensities of all three body sound signal s components, i.e. s_C , s_R , and s_S (simulated snoring), were experimentally investigated by Kaniusas *et al.*⁵ for comparison and for their optimum detection. For this purpose, acoustic sound recordings were carried out with the body sounds sensor (Fig. 1) on two healthy male subjectsⁱⁱ in the supine position.

As shown in Fig. 17, the sound intensities were assessed in 10 homologous chest regions (around third, fifth, and seventh intercostal space (IS) anterior left and right, respectively; fifth and seventh IS lateral left and right, respectively) and on the neck (collateral to the trachea). The heart region around the fifth IS on the anterior left was declared as the “standard” detection region. Therefore, all other eleven regions will be referred to as “alternative” regions. In particular, the “standard” region was investigated in comparison with the “alternative” regions.

The assessed sound level s_{dB} was defined as logarithm of s and its components, respectively. Each subfigure in Fig. 17 includes averaged data on s_{dB} pertaining to s_C , s_R , and s_S . The sound levels in the “alternative” regions are given in relation to the “standard” region ($s_{dB} = 0$).

It can be observed that the “standard” heart region is characterized by similar intensities of s_C and s_S which was approximately 5dB stronger according to Fig. 17(c). This yields a ratio 0dB:+5dB between s_C and s_S , which favors the simultaneous detection of these two components. Conversely, component s_R is rather weak, its intensity tending to be approximately 30dB below that of s_C (Fig. 17(b)). The resulting unfavorable ratio 0dB:−30dB complicates a synchronous auscultation of respiration, cessation of which represents a key parameter for the detection of apneas (see Footnote b).

ⁱⁱIt should be noted that healthy males hardly represent typical apnea patients, especially concerning the snoring sounds. In particular, the simulated snoring of healthy males differs markedly from the obstructive snoring of apnea patients (Sec. 2.3).

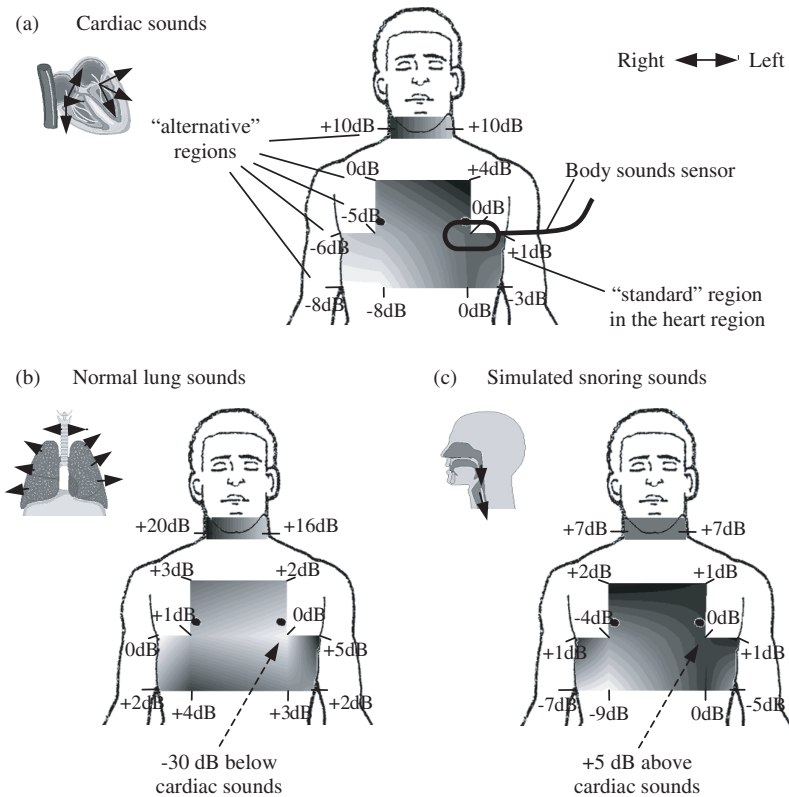


Fig. 17. Local intensity variations of body sounds. Signal amplitudes s_{dB} at “alternative” regions on the chest and neck are given in relation to the “standard” heart region ($s_{dB} = 0$). Values between the measured points are generated using bilinear interpolation and are indicated through the gray tone map. (a) Cardiac sounds s_C . (b) Respiratory sounds s_R . (c) Simulated snoring sounds s_S . The dashed arrows indicate that s_R is 30 dB below s_C at the “standard” region while s_S is 5 dB above s_C .

Aiming for comparisons of regional distributions and more balanced intensities, “alternative” regions should be considered. We see the following tendencies:

- (i) The intensity of s_C decreases with increasing distance from the heart, i.e. it shows minimum values of about -8 dB in the lower right thorax region (Fig. 17(a)). Conversely, it shows a 10 dB maximum at the neck.
- (ii) s_R shows only slight local differences at the thorax (Fig. 17(b)), which result from the distributed sources. Strongly enhanced signals arise at the neck (up to $+20$ dB). Contrary to the discussed asymmetric transmission of the vesicular lung sounds, no evident lateralization of s_R can be observed.
- (iii) s_S shows a maximum of about $+7$ dB at the neck (Fig. 17(c)), as can be expected in view of the source localization. The intensity decreases with increasing distance, reaching a -9 dB minimum in the lower right thorax region.

The experimental results show that optimum auscultation of all three sound components s_C , s_R , and s_S is not to be expected from the “standard” heart region due to the already mentioned ratio $0\text{ dB}:-30\text{ dB}:+5\text{ dB}$ between the respective components. A more efficient auscultation of s_R or a better balance results for the lower right thorax region around the seventh IS which yields a ratio $-8\text{ dB}:-26\text{ dB}:-4\text{ dB}$, or related to the cardiac region $0\text{ dB}:-18\text{ dB}:+4\text{ dB}$. Another attractive auscultation region would be the neck, the right side yielding a ratio $+10\text{ dB}:-10\text{ dB}:+12\text{ dB}$ or $0\text{ dB}:-20\text{ dB}:+2\text{ dB}$, respectively. As can be seen, the minimum of the intensity of s_R cannot be fully overcome.

All the different components of the body sounds prove to contain spatial information that can be easily assessed using simultaneous sound recordings at different body sites. The use of this spatial information may lead to advanced diagnoses^{jj} methods beyond simple single spot sound auscultation, which has already been proposed for both heart sounds⁶⁹ and lung sounds.¹⁸ For instance, in the case of the vesicular lung sounds, acoustic images of a pathologically consolidated lung differ substantially from the images of the healthy lung allowing to localize the abnormality.¹⁸ As a practical restriction, the spatial resolution cannot be expected to resolve differences below approximately 2 cm ($\lambda \approx 2.3\text{ cm}$ at $v = 23\text{ m/s}$, Sec. 4.1.1) in the localization of the sound sources.

6. Concluding Remarks

Acoustical signals of human biomechanical systems reveal mainly three sound components, namely heart sounds, lung sounds, and snoring sounds. The heart sounds occur predominantly because of the valvular activity of the heart. The generation mechanisms of the lung sounds rely on more complicated biomechanical phenomena. In particular, the tracheobronchial sounds are primarily related to the turbulent airflow and vibrations of the upper airway walls, while the vesicular sounds arise mainly during inspiration, as the air moves from larger airways into smaller ones, hitting the branches of the airways. The snoring sounds are mainly generated by vibrations of the pharyngeal walls and the soft palate.

Given the generation mechanisms of the different body sounds, the hypothetical sources of the heart sounds, tracheobronchial lung sounds, and snoring sounds can be considered, in an approximation, as remaining locally restricted to the heart region, the larger airways, and the upper airways, respectively. Contrary to the latter body sounds, the sources of the vesicular lung sounds are not confined to a certain region but are rather distributed within the whole periphery of the lung.

^{jj}It is interesting to note that ultrasound methods, i.e. the most prominent spatial imaging methods using acoustic signals of high frequency (MHz range), have not been successfully applied for imaging of the lung parenchyma, primarily because the sound damping of the parenchyma is prohibitively high at the ultrasound frequencies (see frequency dependence of α in Sec. 4.2.1).⁶³

In contrast to the heart sounds, the lung and snoring sounds exhibit a high variability from one subject to the other and even from one breath to the next. In addition, the different body sounds cannot be considered as being independent. The arising manifold interrelations in between can be attributed to direct mechanical interrelations between the respective sound sources, neural implications, and indirect effects.

The biomechanical propagation mechanisms of the body sounds reveal that a large percentage of the original sound energy never reaches the surface because of spreading, absorption, scattering, reflection, and refraction losses. In particular, the sound attenuation within the body is highly inhomogeneous due to the heterogeneous thorax composition, and it increases generally with increasing sound frequency. There represents the adipose tissue the strongest sound absorber, whereas the strong lowpass characteristics of the lung should be mentioned as well.

Interestingly, the spatial propagation pathway of the sound waves depends on their frequency; that is, the low frequency sounds are predominantly bound to the inner mediastinum, while the high frequency sounds tend to take an airway bound route. The different pathways have a strong influence on the resulting sound propagation velocity and sound wavelength. In particular, the resulting wavelength determines the type of acoustic field (near or far) on the auscultation site and, on the other hand, the strength of the prevailing scattering, reflection, and refraction effects.

The largest reflection losses arise at the tissue-air passage showing a strong mechanical/acoustical impedance mismatch which impedes an efficient sound auscultation. On the other hand, the concurrent refraction yields a flattened wave front in the air, which favors the auscultation.

The regional distribution of the intensity of the surface sounds (accessible through the auscultation) is highly non-uniform and asymmetric, as well as the spatial distribution of the hypothetical sound sources. This is because the sound generation mechanisms lack spatial symmetry, and the spatial transmission pathways are highly inhomogeneous. As an important property, the strong asymmetry arises only for the lower sound frequencies, which can be explained by the frequency dependant propagation pathways of the body sounds.

The regional mappings of the different body sounds show that the intensity of the heart sounds decreases in the thorax region with increasing distance from the heart, as could be expected from the hypothetical sound sources. However, an absolute maximum is given at the neck, which could be explained by close proximity of the auscultation site to the carotid artery. The intensities of the lung sounds in the different thorax regions yield practically no systematic differences in their amplitude, primarily because the vesicular sounds show distributed sources; however, the intensity increases dramatically at the neck, where the bronchial sounds prevail. Lastly, the snoring sound intensity decreases with increasing distance from the neck, as the relevant sound source is located there. Generally, the regional mappings suggest the right thorax region in the area of the seventh intercostal

space or the neck to be optimal regions for the simultaneous auscultation of all three types of the body sounds.

Obviously, the relevant sound generation mechanisms in combination with the transmission properties of the body structures and those of the recording system determine the signal properties of the auscultated body sounds. The heart sounds show spectral components in the [0,100] Hz range, the latter components being statistically irrelevant for the lung and snoring sounds. The spectral components of the lung sounds are in the range up to approximately 500 Hz. The snoring sounds exhibit an extremely high variance of their intensity and spectral composition. Normal snoring appears in the range up to approximately 1000 Hz, while obstructive snoring shows amplitudes up to 2000 Hz.

The presented issues pertaining to the biomechanical generation of the body sounds reveal clinically relevant correlations between the physiological phenomena under investigation and the registered biosignals. The analysis of the unique sound transmission from the sound source to the auscultation site offers a solid basis for both proper understanding of the biosignal relevance and optimization of the recording techniques.

Acknowledgments

This work was supported by the Austrian Federal Ministry of Transport, Innovation and Technology, GZ 140.594/2-V/B/9b/2000. I would like to thank Prof. H. Pfützner and Dipl.-Ing. J. Kosel for valuable comments.

References

1. M. B. Rappaport and H. B. Sprague, *Am. Heart J.* (1941) 257.
2. M. Abella, J. Formolo and D. G. Penney, *J. Acoust. Soc. Am.* (1992) 2224.
3. P. Y. Ertel, M. Lawrence and W. Song, *J. Audio Eng. Soc.* (1971) 182.
4. R. Loudon and R. L. H. Murphy, *Am. Rev. Respir. Dis.* (1984) 663.
5. E. Kaniusas, H. Pfützner and B. Saletu, *IEEE Trans. Biomed. Eng.* (2005) 1812.
6. B. Saletu and M. Saletu-Zyhlarz, eds., *What You Always Wanted to Know About the Sleep (in German)* (Ueberreuter Publisher, Vienna, 2001).
7. I. Veit, ed., *Technical Acoustics (in German)* (Vogel Publisher, Würzburg, 1996).
8. P. Y. Ertel, M. Lawrence, R. K. Brown and A. M. Stern, *Circulation* (1966) 889.
9. P. Y. Ertel, M. Lawrence, R. K. Brown and A. M. Stern, *Circulation* (1966) 899.
10. P. J. Hollins, *Br. J. Hosp. Med.* (1971) 509.
11. R. M. Rangayyan, ed., *Biomedical Signal Analysis: A Case-Study Approach* (Wiley-IEEE Press, 2002).
12. D. Barschdorff, S. Ester and E. Most, in *Comparative Approaches to Medical Reasoning*, eds. M. E. Cohen and D. L. Hudson (World Scientific Publishing, 1995), p. 271.
13. University of Wales, College of Medicine, *Cardiac Auscultation Site* (http://mentor.uwcm.ac.uk:11280/aspire/cardiac_auscultation/notes/part_2/the_audio_section/,2005).
14. C. Lessard and M. Jones, *Innov. Technol. Biol. Med.* (1988) 116.

15. L. J. Hadjileontiadis and S. M. Panas, *IEEE Trans. Biomed. Eng.* (1997) 642.
16. H. Pasterkamp, S. S. Kraman and G. R. Wodicka, *Am. J. Respir. Crit. Care Med.* (1997) 974.
17. F. Dalmay, M. T. Antonini, P. Marquet and R. Menier, *Eur. Respir. J.* (1995) 1761.
18. M. Kompis, H. Pasterkamp and G. R. Wodicka, *Chest* (2001) 1309.
19. P. Fachinger, *Computer Based Analysis of Lung Sounds in Patients with Pneumonia — Automatic Detection of Bronchial Breathing by Fast-Fourier-Transformation (in German)* (Dissertation, Philipps-University Marburg, 2003).
20. McGill University, Faculty of Medicine, *Molson Medical Informatics Student Projects* (<http://sprojects.mmip.mcgill.ca/mvs/>, 2005).
21. L. J. Hadjileontiadis and S. M. Panas, in *Proceedings of the 18th Annual EMBS International Conference* (IEEE, 1996), p. 2217.
22. L. J. Hadjileontiadis and S. M. Panas, *IEEE Trans. Biomed. Eng.* (1997) 1269.
23. V. K. Iyer, P. A. Ramamoorthy and Y. Ploysongsang, *IEEE Trans. Biomed. Eng.* (1989) 1133.
24. A. Jones, R. D. Jones, K. Kwong and Y. Burns, *Phys. Ther.* (1999) 682.
25. R. Ferber, R. Millman, M. Coppola, J. Fleetham, C. F. Murray, C. Iber, V. McCall, G. Nino-Murcia, M. Pressman, M. Sanders, K. Strohl, B. Votteri and A. Williams, *Sleep* (1994) 378.
26. G. R. Wodicka, K. N. Stevens, H. L. Golub, E. G. Cravalho and D. C. Shannon, *IEEE Trans. Biomed. Eng.* (1989) 925.
27. G. Liistro, D. Stanescu and C. Veriter, *J. Appl. Physiol.* (1991) 2736.
28. K. Wilson, R. A. Stoohs, T. F. Mulrooney, L. J. Johnson, C. Guilleminault and Z. Huang, *Chest* (1999) 762.
29. R. Beck, M. Odeh, A. Oliven and N. Gavriely, *Eur. Respir. J.* (1995) 2120.
30. F. Cirignota, *Min. Med. Rev.* (2004) 177.
31. J. R. Perez-Padilla, E. Slawinski, L. M. Difrancesco, R. R. Feige, J. E. Remmers and W. A. Whitelaw, *Am. Rev. Respir. Dis.* (1993) 635.
32. F. Series, I. Marc and L. Atton, *Chest* (1993) 1769.
33. B. Truax, ed., *Handbook for Acoustic Ecology* (Cambridge Street Publishing, 1999).
34. J. Schäfer, *Laryngol. Rhinol. Otol.* (1988) 449.
35. J. Schäfer, ed., *Snoring, Sleep Apnea, and Upper Airways (in German)* (Georg Thieme Publisher, 1996).
36. Y. Itasaka, S. Miyazaki, K. Ishikawa and K. Togawa, *Psychiat. Clin. Neurosci.* (1999) 299.
37. M. Moerman, M. De Meyer and D. Pevernagie, *Acta Otorhinolaryngol. Belg.* (2002) 113.
38. J. Cummiskey, T. C. Williams, P. E. Krumpe and C. Guilleminault, *Am. Rev. Respir. Dis.* (1982) 221.
39. K. M. Hartse, V. C. Thessing, G. H. Branham and J. F. Eisenbeis, *Sleep Res.* (1995) 243.
40. P. E. Krumpe and J. M. Cummiskey, *Am. Rev. Respir. Dis.* (1980) 797.
41. D. L. Brunt, K. L. Lichstein, S. L. Noe, R. N. Aguillard and K. W. Lester, *Sleep* (1997) 1151.
42. W. Hida, H. Miki, Y. Kikuchi, C. Miura, N. Iwase, Y. Shimizu and T. Takishima, *Tohoku J. Exp. Med.* (1988) 137.
43. T. N. Liesching, C. Carlisle, A. Marte, A. Bonitati, R. P. Millman, *Chest* (2004) 886.
44. E. Kaniusas, L. Mehnen, H. Pfützner, B. Saletu and R. Popovic, in *Proceedings of International Measurement Confederation*, eds. A. Afjehi-Sadat, M. N. Durakbasa and P. H. Osanna (Austrian Society for Measurement and Automation, 2000), p. 177.

45. A. W. McCombe, V. Kwok and W. M. Hawke, *Clin. Otolaryngol.* (1995) 348.
46. T. Verse, W. Pirsig, B. Junge-Hülsing and B. Kroker, *Chest* (2000) 1613.
47. H. Rauscher, W. Popp and H. Zwick, *Eur. Respir. J.* (1991) 655.
48. T. Penzel, G. Amend, K. Meinzer, J. H. Peter and P. Wichert, *Sleep* (1990) 175.
49. C. A. Kushida, S. Rao, C. Guilleminault, S. Giraudo, J. Hsieh, P. Hyde and W. C. Dement, *Sleep Res. Online* (1999) 7.
50. M. Sergi, M. Rizzi, A. L. Comi, O. Resta, P. Palma, A. De Stefano and D. Comi, *Sleep Breath.* (1999) 47.
51. M. Karam, R. A. Wise, T. K. Natarajan, S. Permutt and H. N. Wagner, *Circulation* (1984) 866.
52. S. Silbernagl and A. Despopoulos, eds., *Pocket-Atlas of Physiology (in German)* (Georg Thieme Publisher, Stuttgart, 1991).
53. C. O. Olsen, G. S. Tyson, G. W. Maier, J. W. Davis and J. S. Rankin, *Circulation* (1985) 668.
54. A. Guz, J. A. Innes and K. Murphy, *J. Physiol.* (1987) 499.
55. M. Elstad, K. Toska, K. H. Chon, E. A. Raeder and R. J. Cohen, *J. Physiol.* (2001) 251.
56. K. Ishikawa and T. Tamura, *Angiology* (1979) 750.
57. W. R. Milnor, ed., *Hemodynamics* (Williams & Wilkins Publisher, Baltimore, 1989).
58. T. J. Pedley, ed., *The Fluid Mechanics of Large Blood Vessels* (Cambridge University Press, Cambridge, 1980).
59. F. Trendelenburg, ed., *Introduction into Acoustic (in German)* (Springer Publisher, Berlin, 1961).
60. D. A. Rice, *J. Appl. Physiol.* (1983) 304.
61. E. Meyer and E. G. Neumann, eds., *Physical and Technical Acoustic (in German)* (Vieweg Publisher, Braunschweig, 1975).
62. A. Bulling, F. Castrop, J. D. Agneskirchner, W. A. Ovtcharoff, L. J. Wurzinger and M. Gratzl, *Body Explorer* (Springer Publisher, CD-ROM, 1997).
63. M. Kompis, H. Pasterkamp, Y. Oh, Y. Motai and G. R. Wodicka, in *Proceedings of the 20th annual EMBS International Conference* (IEEE, 1998), p. 1661.
64. K. R. Erikson, F. J. Fry and J. P. Jones, *IEEE Trans. Son. Ultrason.* (1974) 144.
65. J. B. Calvert, *Sound Waves* (University of Denver, <http://www.du.edu/~jcalvert/waves/soundwav.htm>, 2000).
66. P. D. Welsby and J. E. Earis, *Postgrad. Med. J.* (2001) 617.
67. P. D. Welsby, G. Parry and D. Smith, *Postgrad. Med. J.* (2003) 695.
68. H. Pasterkamp, S. Patel and G. R. Wodicka, *Med. Biol. Eng. Comput.* (1997) 103.
69. D. Leong-Kon, L. G. Durand, J. Durand and H. Lee, in *Proceedings of the 20th annual EMBS International Conference* (IEEE, 1998), p. 17.